



This discussion paper is/has been under review for the journal Atmospheric Chemistry and Physics (ACP). Please refer to the corresponding final paper in ACP if available.

# A multi-year study of lower tropospheric aerosol variability and systematic relationships from four North American regions

J. P. Sherman<sup>1</sup>, P. J. Sheridan<sup>2</sup>, J. A. Ogren<sup>2</sup>, E. A. Andrews<sup>2</sup>, L. Schmeisser<sup>2</sup>, A. Jefferson<sup>2</sup>, and S. Sharma<sup>3</sup>

<sup>1</sup>Dept. Physics and Astronomy, Appalachian State University, 525 Rivers St, CAP Building Room 231, Boone, NC, 28608, USA

<sup>2</sup>NOAA, Earth Systems Research Laboratory, Global Monitoring Division/GMD-1, 325 Broadway, Boulder, CO, 80305, USA

<sup>3</sup>Environment Canada, 4905 Dufferin St, Toronto, ON, M3H 5T4, Canada

Received: 28 September 2014 – Accepted: 10 October 2014 – Published: 28 October 2014

Correspondence to: J. P. Sherman (shermanjp@appstate.edu)

Published by Copernicus Publications on behalf of the European Geosciences Union.

**A multi-year study of lower tropospheric aerosol variability and systematic relationships**

J. P. Sherman et al.

Title Page

Abstract

Introduction

Conclusions

References

Tables

Figures

◀

▶

◀

▶

Back

Close

Full Screen / Esc

Printer-friendly Version

Interactive Discussion



## Abstract

Hourly-averaged aerosol radiative properties measured over the years 2010–2013 at four continental North American NOAA/ESRL Federated Aerosol Network sites – Southern Great Plains in Lamont, OK (SGP), Bondville, IL (BND), Appalachian State University in Boone, NC (APP), and Egbert, Ontario, Canada (EGB) were analyzed to determine regional variability and temporal variability on several timescales, how this variability has changed over time at the long-term sites (SGP and BND), and whether systematic relationships exist for key aerosol properties relevant to radiative forcing calculations. The aerosol source types influencing the four sites differ enough so as to collectively represent rural, anthropogenically-perturbed air conditions over much of continental North America.

Seasonal variability in scattering and absorption coefficients at 550 nm ( $\sigma_{sp}$  and  $\sigma_{ap}$ , respectively) and most aerosol intensive properties was much larger than day of week and diurnal variability at all sites for both the sub-10  $\mu\text{m}$  and sub-1  $\mu\text{m}$  aerosols. Pronounced summer peaks in scattering were observed at all sites, accompanied by broader peaks in absorption, higher single-scattering albedo ( $\omega_0$ ), and lower hemispheric backscatter fraction ( $b$ ). Amplitudes of diurnal and weekly cycles in absorption at the sites were larger for all seasons than those of scattering. The cycle amplitudes of intensive optical properties on these shorter timescales were minimal in most cases. In spite of the high seasonality in  $\omega_0$  and  $b$ , the co-variation of these two intensive properties cause the corresponding seasonal cycle in monthly median direct radiative forcing efficiency to be small, with changes of only a few percent at all sites.

Median sub-10  $\mu\text{m}$  aerosol  $\sigma_{sp}$  values for SGP and BND for the 2010–2013 time period were  $\sim 25\%$  lower for all months than during the late 1990s period studied by Delene and Ogren (2002), consistent with the trends reported in other North American studies. There were even larger reductions in sub-1  $\mu\text{m}$  aerosol  $\sigma_{sp}$ , leading to a larger coarse-mode influence at both sites. Similar reductions in median  $\sigma_{ap}$  were observed at BND but median  $\sigma_{ap}$  changed little at SGP relative to the earlier observations of

## A multi-year study of lower tropospheric aerosol variability and systematic relationships

J. P. Sherman et al.

Title Page

Abstract

Introduction

Conclusions

References

Tables

Figures

◀

▶

◀

▶

Back

Close

Full Screen / Esc

Printer-friendly Version

Interactive Discussion





## A multi-year study of lower tropospheric aerosol variability and systematic relationships

J. P. Sherman et al.

Title Page

Abstract

Introduction

Conclusions

References

Tables

Figures

◀

▶

◀

▶

Back

Close

Full Screen / Esc

Printer-friendly Version

Interactive Discussion

addition to relationships among some of these properties. The US-based Interagency Monitoring of Protected Visual Environments network (IMPROVE, Malm et al., 2004) has conducted similar studies using speciated aerosol mass concentrations, light scattering (at some sites), and reconstructed light extinction measurements in remote areas of the US. Recent long-term trend studies based on data from surface networks indicate that aerosol optical depth (Li et al., 2014; Yoon, 2012) and lower tropospheric light scattering (Collaud-Coen et al., 2013) have decreased at a majority of North American aerosol monitoring sites. Hand et al. (2014) reported large reductions of up to 50 % in reconstructed aerosol visible light extinction for the 20 % haziest days annually at IMPROVE sites in the US from 2002–2011, with the largest decreases in the eastern US. Through trend analysis of speciated aerosol mass concentrations and emissions inventories, they showed that reductions in SO<sub>2</sub> emissions (produced largely by coal-burning power plants) have likely played a major role in the reduced aerosol light extinction, particularly in the eastern US. Murphy et al. (2011) applied trend analysis using IMPROVE sites across the US to show that elemental carbon aerosol mass concentrations decreased by over 25 % between 1990–2004, with reductions during winter months close to 50 %. Region and season-dependent changes in emissions of aerosols and precursor gases may result in changes in mean values and variability of aerosol optical and micro-physical properties, but few long-term studies of aerosol intensive properties (i.e., properties that are independent of aerosol loading, such as single scattering albedo, asymmetry parameter, and direct radiative forcing efficiency) conducted over multiple regions have ever been performed in North America.

Surface-based networks employing in situ methods, such as the NOAA/ESRL Federated Aerosol Network, are particularly well-suited for studies of aerosol variability on a variety of temporal scales under both clear and cloudy conditions. An additional advantage is the ability to derive single-scattering albedo ( $\omega_0$ ) under low aerosol loading conditions. Single-scattering albedo derived from sky radiance measurements made by Cimel sun/sky radiometers as part of AERONET possess high uncertainties for lower aerosol optical depths typical of most rural North American sites (Dubovik et al., 2000).

**A multi-year study of lower tropospheric aerosol variability and systematic relationships**

J. P. Sherman et al.

Title Page

Abstract

Introduction

Conclusions

References

Tables

Figures

◀

▶

◀

▶

Back

Close

Full Screen / Esc

Printer-friendly Version

Interactive Discussion

A weakness of many in situ surface aerosol measurement systems is the inability to determine the hygroscopic dependence of aerosol light scattering. Many aerosol monitoring stations in the NOAA/ESRL and Global Atmosphere Watch (GAW) networks follow similar sampling protocols where the aerosols are dried to decouple the aerosol properties from their dependence on relative humidity (RH). Another concern is the uncertainty as to when and under what conditions the near-surface measurements are representative of the atmospheric column at each site. The first problem can be addressed through the use of humidified light scattering measurements (e.g., Sheridan et al., 2001), which are or have been made at a few ESRL network sites, including three of the four sites reported in this paper. The second issue has been investigated through multi-year aircraft measurement programs over instrumented surface sites. At the Southern Great Plains (SGP, near Lamont, OK) and Bondville (BND), IL sites respectively, Andrews et al. (2004) and Sheridan et al. (2012) have reported that median values of key dried aerosol intensive optical properties such as  $\omega_0$  and scattering Ångström exponent ( $\alpha_{sp}$ ) show little statistical variability up to  $\sim 2$  km altitude and that long-term median values can be well-approximated by the near-surface values, even though instantaneous measurements of the near-surface properties are often poorly correlated with those of the column.

Delene and Ogren (2002) (hereafter referred to as D&O2002) reported multi-year measurements of aerosol optical properties at four North American sites that were used to (1) highlight the need to quantify both aerosol extensive properties (i.e., properties that depend on aerosol amount) and intensive properties on regional scales over at least a 1 year period; and (2) conclude that global measurements of aerosol optical depth (denoted by AOD or  $\tau$ ) made daily by satellites, combined with in situ measurements of regionally-representative aerosol intensive properties, are likely sufficient to determine aerosol direct radiative forcing with a relatively small amount of uncertainty. One drawback of their study was the then-lack of NOAA/ESRL Federated Network sites in the eastern portion of North America, where population and aerosol loading is highest. D&O2002 also studied systematic relationships between aerosol



---

**A multi-year study of lower tropospheric aerosol variability and systematic relationships**J. P. Sherman et al.

---

[Title Page](#)[Abstract](#)[Introduction](#)[Conclusions](#)[References](#)[Tables](#)[Figures](#)[◀](#)[▶](#)[◀](#)[▶](#)[Back](#)[Close](#)[Full Screen / Esc](#)[Printer-friendly Version](#)[Interactive Discussion](#)

3. Are there systematic relationships between these optical properties? How do these relationships vary with region and with season?

This study differs from the D&O2002 paper in three respects:

1. The time period of the study is different, which allows for us to compare (at least for BND and SGP) how the optical properties have changed.
2. This paper has a focus on continental sites, whereas D&O2002's four sites included an Arctic site and a marine site.
3. Aerosol temporal variability and systematic relationships between aerosol optical properties are investigated as a function of season. D&O2002 only looked at annual systematic variability.

## 2 Methodology

### 2.1 Site descriptions

All four sites in this study are mid-latitude (35–45° N) locations in North America with elevations ranging from 230 to 1080 m a.s.l., placing them firmly in the boundary layer. These sites can be categorized as anthropogenically-perturbed, rural continental locations, distant from both large population centers and significant emissions sources and thus representative of regional atmospheric conditions. BND is located near a regional population center (Sect. 2.1.3) that lies predominately downwind of the site, justifying the same categorization as the other sites. Table 2 and the sections below provide additional details about each location.

#### 2.1.1 Lamont, Oklahoma, USA (SGP)

SGP is the Department of Energy's Cloud, Aerosol and Radiation Testbed (CART) site and is located in north central Oklahoma near the town of Lamont (pop. 417) in







timescales less than one hour so it is assumed that the same aerosols are sampled for both size cuts at these switching rates over a large majority of hours. The EGB system used a 1  $\mu\text{m}$  URG cyclone to achieve a permanent  $D_p < 1 \mu\text{m}$  particle size cut so  $\text{PM}_{10}$  aerosol properties are not available for EGB. Descriptions of the basic inlet design and sampling strategy, including flow rates, tubing sizes and estimated aerosol losses, have been provided elsewhere (Sheridan et al., 2001; D&O2002).

## 2.2 Measurements and instruments

This study used several primary aerosol measurements (Table 2), including aerosol light scattering ( $\sigma_{\text{sp}}$ ), hemispheric backscattering ( $\sigma_{\text{bsp}}$ ), and absorption ( $\sigma_{\text{ap}}$ ) coefficients. All of these parameters were measured for both the  $\text{PM}_{10}$  and  $\text{PM}_1$  size ranges (only  $\text{PM}_1$  for EGB) so that the fractional radiative effects of sub-1  $\mu\text{m}$  particles ( $\text{PM}_1$ ) could be estimated.

A three-wavelength (3- $\lambda$ ) integrating nephelometer (Model 3563, TSI Inc., St. Paul, MN) was used at all sites for measurement of the total light scattering coefficients (angular range of 7–170°) and hemispheric backscattering coefficients (angular range of 90–170°). The operating wavelengths for the instruments used in this study are given in Table 2. Measurement details and uncertainties for the TSI nephelometer have been described elsewhere (e.g., Anderson et al., 1999; Sheridan et al., 2002). Aerosol properties at these locations (e.g.,  $\omega_0 > 0.7$  and minor coarse mode fractions, as discussed by Massoli et al., 2009) were such that the widely-used nephelometer correction (e.g., truncation) scheme of Anderson and Ogren (1998) was considered appropriate and applied in this study.

The aerosol light absorption coefficients were determined with filter-based instruments that make measurements at wavelengths close to those of the TSI nephelometer. The majority of these measurements were made with 3- $\lambda$  Particle Soot Absorption Photometers (PSAP, Radiance Research, Seattle, WA). PSAP measurements were corrected for sample area, flow rate, and non-idealities in the manufacturer's calibration as described in Bond et al. (1999) and Ogren (2010). Measurement uncertainties for

## A multi-year study of lower tropospheric aerosol variability and systematic relationships

J. P. Sherman et al.

Title Page

Abstract

Introduction

Conclusions

References

Tables

Figures

◀

▶

◀

▶

Back

Close

Full Screen / Esc

Printer-friendly Version

Interactive Discussion



## A multi-year study of lower tropospheric aerosol variability and systematic relationships

J. P. Sherman et al.

Title Page

Abstract

Introduction

Conclusions

References

Tables

Figures

◀

▶

◀

▶

Back

Close

Full Screen / Esc

Printer-friendly Version

Interactive Discussion

the PSAP have been described in detail elsewhere (Anderson et al., 1999; Bond et al., 1999; Sheridan et al., 2002). The EGB station was an exception in that it had a single wavelength (1- $\lambda$ ) PSAP instrument operating continuously over its entire data record. Absorption Ångström exponent values were used to adjust the PSAP light absorption measurements to the nephelometer wavelengths for calculating intensive aerosol properties (Table 1). The PSAPs were modified by placing a small ( $\sim 5$  W) heater on their internal inlet lines at the connection with the optical block. The heating was gentle, typically only a few degrees, but the temperature of the metal block was kept elevated above the incoming sample air temperature so the RH of the sample and reference filters stayed relatively low. The heater was not actively controlled to maintain a specific RH, but RH variability at low RH is not believed to influence the measurements as strongly as RH variability at high RH (Anderson et al., 2003). Tests suggest that the heater kept the RH at the filters below 40 % most of the time. An RH of 50 % at the filter would have been exceeded only during sampling of very humid air (Sheridan et al., 2012).

A new light absorption instrument (Continuous Light Absorption Photometer, CLAP) was recently developed by NOAA/ESRL to eventually replace the PSAP at all stations in the NOAA network (Ogren et al., 2013). The CLAP is similar to the PSAP in that particles are collected on a filter of the same material as used in the PSAP and light transmission through the filter is monitored continuously. The CLAP differs from the PSAP in that instead of a single sample spot, it has eight sample spots, which are selected by solenoids that switch to the next sample spot once the filter transmittance reaches a desired limit (typically 0.7). Thus, the CLAP can run eight times as long as the PSAP before requiring a filter change, ideal for remote sites which aren't visited daily or for highly polluted sites. The designed similarity with the PSAP means that the same corrections (Bond et al., 1999; Ogren, 2010) can be applied. After running for an extended overlap period with the CLAP at the BND station, the PSAP was removed in March 2012, so the final 21 months of light absorption measurements at BND were made with a CLAP. The PSAP/CLAP comparisons made during the overlap period at

BND indicate that the CLAP measures light absorption at all wavelengths about 5% lower on average than the PSAP. The CLAP comes with a small heater built in and is controlled to a set temperature, typically 39 °C to minimize RH effects during sampling.

The primary measurements (Table 2) such as  $\sigma_{sp}$ ,  $\sigma_{bsp}$ , and  $\sigma_{ap}$  were used to derive several aerosol properties (Table 1) used in radiative transfer calculations (Haywood and Shine, 1995) and other aerosol studies. These properties have been described in many previous papers (e.g., Sheridan et al., 2001; D&O2002) so only a brief discussion follows. The light extinction coefficient ( $\sigma_{ep}$ ) is the sum of the scattering and absorption coefficients. The primary measurements (plus  $\sigma_{ep}$ ) are extensive parameters, as they depend on the amount of aerosol present. The single-scattering albedo ( $\omega_0$ ) is the fraction of extinction due to scattering, with lower values of  $\omega_0$  corresponding to more absorbing aerosols. The hemispheric backscatter coefficient ( $b$ ) represents the fraction of light scattered into the backward hemisphere in the nephelometer and provides qualitative information on aerosol size, with larger values of  $b$  most often corresponding to smaller particles. The scattering and absorption Ångström exponents ( $\alpha_{sp}$  and  $\alpha_{ap}$ ) describe the wavelength dependence of light scattering and absorption, respectively. The scattering Ångström exponent ( $0 \leq \alpha_{sp} \leq 4$ ) provides semi-quantitative information regarding the aerosol size distribution, with larger values of  $\alpha_{sp}$  corresponding to size distributions dominated by smaller particles (van de Hulst, 1957). The absorption Ångström exponent can provide information on aerosol type for certain aerosols (e.g., Costabile et al., 2013; Bergstrom et al., 2007). For example, dust and some organics absorb light strongly in the near-UV and blue-violet regions of the electromagnetic spectrum (the so-called “brown carbon”), corresponding to  $\alpha_{ap} > 1$  (Costabile et al., 2013). Absorption by black carbon (BC) decreases as  $\lambda^{-1}$  in the near-UV through near-IR, corresponding to  $\alpha_{ap} = 1$  (Bergstrom et al., 2007). The sub-1  $\mu\text{m}$  scattering and absorption fractions  $R_{sp}$  and  $R_{ap}$ , respectively, indicate the fractions of  $\text{PM}_{10}$  light scattering and absorption due to  $\text{PM}_1$  particles and serve as a rough proxy for the “fine-mode” fraction of scattering and absorption. Haywood and Shine (1995) present simple equations for calculating top-of-atmosphere (TOA) aerosol direct radiative forc-

## A multi-year study of lower tropospheric aerosol variability and systematic relationships

J. P. Sherman et al.

Title Page

Abstract

Introduction

Conclusions

References

Tables

Figures

◀

▶

◀

▶

Back

Close

Full Screen / Esc

Printer-friendly Version

Interactive Discussion



## A multi-year study of lower tropospheric aerosol variability and systematic relationships

J. P. Sherman et al.

Title Page

Abstract

Introduction

Conclusions

References

Tables

Figures

◀

▶

◀

▶

Back

Close

Full Screen / Esc

Printer-friendly Version

Interactive Discussion



ing (DRF) and direct radiative forcing efficiency (DRFE, Table 1) for an optically-thin, partially-absorbing atmosphere. DRFE represents the DRF per unit aerosol optical depth (referenced in the literature as AOD or  $\tau$ ) and is to first-order independent of  $\tau$ . If globally-averaged values for all non-aerosol parameters are used (Table 1), the simple equation for DRFE provides a means of comparing the intrinsic forcing efficiency of the aerosols measured at different sites and times, through its dependence on  $\omega_0$  and on up-scatter fraction  $\beta$ . The up-scatter fraction represents the fraction of incoming solar radiation that is scattered by atmospheric aerosols back to space, and has been related to the measured parameter  $b$  by the approximation of Wiscombe and Grams (1976). A second-order curve fit of the points in their Fig. 3 as reported in Sheridan and Ogren (1999) provides the parameterization shown in Table 1.

### 2.3 Data consistency

Quality assurance for each site was performed by the site scientist to invalidate measurements affected by instrumental or sampling problems and to eliminate data contaminated by local sources (e.g., short-lived plumes caused by local traffic sources, mowing operations, etc.). Data where the PSAP filter transmission was less than 50 % were also discarded because high filter loading greatly increases the measurement uncertainty (Bond et al., 1999). Details of the quality assurance methods are provided in D&O2002. In addition to being measured at low RH, the scattering and absorption measurements were adjusted to standard temperature and pressure ( $T = 273.15$  K,  $P = 101.35$  kPa) to facilitate comparisons among the sites. Only hours for which scattering at 550 nm was at least  $1.0 \text{ M m}^{-1}$  for the  $\text{PM}_{10}$  size cut were used to calculate the aerosol intensive property statistics, so as to reduce noise resulting from taking ratios of two small quantities (see Table 1). This filtering discarded 1 % or fewer of the hours at all sites except SGP, where 3.9 % of the hours were discarded. The lack of  $\text{PM}_{10}$  data from EGB precluded calculation of sub- $1 \mu\text{m}$  aerosol scattering and absorption fractions  $R_{\text{sp}}$  and  $R_{\text{ap}}$  and the use of a single-wavelength PSAP at EGB precluded calculation of absorption Ångström exponent ( $\alpha_{\text{sp}}$ ).

## A multi-year study of lower tropospheric aerosol variability and systematic relationships

J. P. Sherman et al.

Title Page

Abstract

Introduction

Conclusions

References

Tables

Figures

◀

▶

◀

▶

Back

Close

Full Screen / Esc

Printer-friendly Version

Interactive Discussion

The RH inside the nephelometer occasionally exceeded 40 % during the humid summer months (reaching as high as  $\sim 50\%$ ), which can result in a small enhancement of light scattering above “dry” aerosol light scattering levels. To determine the magnitude of this effect, we applied scattering hygroscopic growth gamma fit parameters (Quinn et al., 2005) based on humidified light scattering and hemispheric backscattering measurements at APP and SGP (not included here) to the hourly-averaged light scattering and hemispheric backscattering values for hours when the nephelometer internal RH exceeded 40 %. For gamma values encompassing the 5th through 95th percentiles (i.e., basically the entire range of possible growth factors), the correction of light scattering and hemispheric backscattering from values at the elevated RH to values at RH = 40 % was less than 3–4 % and the uncertainty in applying static correction factors for sites with no humidified scattering measurements (BND, EGB) was similarly small. Based on these relatively small adjustments, hours with elevated nephelometer RH were retained and no RH corrections were applied to the scattering measurements for these hours.

### 3 Results and discussion

Regional and temporal variability of  $PM_{10}$  and  $PM_1$  aerosol properties are presented in Sects. 3.1–3.3. The period of study is 2010–2013 and the measurements were made continuously or near-continuously at all four sites over the full period (Table 2). Section 3.1 presents annual cycles of monthly median aerosol properties at the four sites over this four-year period. Differences in median values among the four sites for the entire period and for individual months were used to quantify regional variability. Comparisons of the annual cycles of aerosol properties at the long-term sites (SGP and BND) for the current period with those of the D&O2002 period and with the intervening years at SGP and BND provide a simple means for examining the influence of length of data set on the annual cycle of aerosol properties and how they have changed over time. Weekly and diurnal cycles of median aerosol properties over the four-year period





## A multi-year study of lower tropospheric aerosol variability and systematic relationships

J. P. Sherman et al.

Title Page

Abstract

Introduction

Conclusions

References

Tables

Figures

◀

▶

◀

▶

Back

Close

Full Screen / Esc

Printer-friendly Version

Interactive Discussion

2009; Link et al., 2014), which enhance the  $PM_1$  scattering values, especially during warm-season months. Land use patterns in the rural continental eastern US are more similar to APP than to SGP or BND, leading us to speculate that  $R_{sp}$  and  $R_{ap}$  values in the rural continental eastern US are probably closer to those of APP than of SGP and BND and that there is likely a west-to-east gradient in the relative influence of  $PM_1$  to aerosol scattering and absorption.

The regional differences for the other aerosol intensive properties in Figs. 1 and 2 over the entire period were, in most cases, much less than the seasonal variability in monthly median values at the individual sites. This result indicates that seasonality must be considered when examining regional differences, at least for the four regions in this study. Similar results were obtained when using means and SDs over the entire study period (not shown), where the differences in most mean aerosol properties between the sites were substantially less than the SDs for the individual sites.

### 3.1.2 Seasonal variability as a function of region

The amplitude of the annual cycle in monthly median  $PM_{10}$  scattering coefficient ( $\sigma_{sp}$ ) was much larger at APP than at SGP and BND, with monthly median  $\sigma_{sp}$  values increasing by a factor of  $\sim 3$  from winter to summer (Fig. 1). EGB exhibited the largest seasonality in  $PM_1 \sigma_{sp}$  and  $\sigma_{ap}$ , with comparable  $PM_1 \sigma_{sp}$  seasonality at APP. Median  $PM_{10}$  and  $PM_1 \sigma_{sp}$  were highest during July and/or August at all sites, followed by sharp decreases in September. All sites also exhibited absorption peaks in summer (typically highest in August) but the absorption peaks tended to be broader than the scattering peaks for all sites except EGB, where the autumn decreases in median  $PM_1 \sigma_{sp}$  and  $\sigma_{ap}$  were similar (factor of  $\sim 3$  to 4). In contrast, the autumn decreases in median  $PM_{10}$  and  $PM_1 \sigma_{sp}$  at APP were twice as large as the autumn decreases in  $\sigma_{ap}$ . SGP and BND represented intermediate cases, with monthly median  $\sigma_{sp}$  decreasing  $\sim 1.5$  times more than median  $\sigma_{ap}$  during autumn. The fact that the scattering and absorption seasonal cycles were different in terms of magnitude and broadness of peak suggests that there were different sources, sinks, and/or atmospheric processes affecting the

**A multi-year study of lower tropospheric aerosol variability and systematic relationships**

J. P. Sherman et al.

Title Page

Abstract

Introduction

Conclusions

References

Tables

Figures

◀

▶

◀

▶

Back

Close

Full Screen / Esc

Printer-friendly Version

Interactive Discussion

aerosol properties observed at each site. Summer-to-fall changes in  $\sigma_{sp}$  and  $\sigma_{ap}$  of similar magnitude at EGB indicate that primary aerosol sources were likely responsible for both the  $\sigma_{sp}$  and  $\sigma_{ap}$  seasonality at EGB while the much larger summer scattering enhancement at APP (relative to that of absorption) is consistent with particle growth dominating the large seasonality in  $\sigma_{sp}$  at APP, as discussed below. Particle growth and some seasonality in primary sources likely contributed to the seasonality in  $\sigma_{sp}$  and  $\sigma_{ap}$  at SGP and BND.

The large amplitudes of the annual  $PM_1$   $\sigma_{sp}$  and  $\sigma_{ap}$  cycles at EGB were primarily influenced by the seasonally-dependent frequency of south/southeasterly flow from the heavily-populated Toronto area and northeastern US (most frequent in spring and summer), for which higher mass concentrations of sulfates, organics, and black carbon (BC) are measured (Chan et al., 2010). Long-range transport of biogenic secondary organic aerosol (SOA) from boreal forests also influenced  $\sigma_{sp}$  at EGB during summer months for northwesterly flow (Chan et al., 2010). During fall and winter, the frequency of transport from the south is less and relatively cleaner northwesterly air masses prevail, resulting in lower scattering and absorption at EGB during these months.

The APP site is largely influenced by biogenic SOA during the warm season (Link et al., 2014) and the sharp autumn decrease in  $\sigma_{sp}$  (Fig. 1) is in agreement with seasonality in biogenic VOC precursor emissions in the SE US (Goldstein et al., 2009), along with reduced photochemistry. The annual cycle in  $\sigma_{sp}$  at APP is qualitatively similar to the seasonality in satellite-based measurements of SE US AOD reported by Goldstein et al. (2009), who showed that both the large seasonality in spatial AOD variability and the AOD dependence on temperature were consistent with SOA formed from biogenic VOC oxidation, mediated by anthropogenic precursor gases. Multi-year measurements reported by the IMPROVE network (Hand et al., 2011) showed that sulfates were the principal component of the surface-level  $PM_{2.5}$  mass fraction for all months at IMPROVE sites in the Appalachian mountain region of the US (with mass fractions of  $\sim 0.6$  during summer) but  $PM_1$  chemical composition measurements made by an Aerodyne Aerosol Mass Spectrometer over two summers and one winter at APP revealed

**A multi-year study of lower tropospheric aerosol variability and systematic relationships**

J. P. Sherman et al.

Title Page

Abstract

Introduction

Conclusions

References

Tables

Figures

◀

▶

◀

▶

Back

Close

Full Screen / Esc

Printer-friendly Version

Interactive Discussion

that a majority of  $PM_1$  non-refractory mass concentration is organic aerosol (Fig. S1 of the Supplement). The discrepancy could be due in part to the higher-elevation of the APP site. Based on aircraft measurements of aerosol composition made using an Aerodyne AMS, Kleinman et al. (2007) reported much higher organic mass fractions above the surface than measured by IMPROVE surface sites in the eastern US. A detailed analysis of the relative roles of sulfates and organics to the measured optical properties is beyond the scope of this paper and will form the topic of a future publication.

A majority of the warm-season  $PM_1$  aerosol mass at SGP consists of low and highly oxidized SOA (corresponding loosely to “fresher”, and “aged” organic aerosol, respectively) as reported by Fast et al. (2013), but the seasonal cycle in  $PM_1 \sigma_{sp}$  at SGP during our study period was much weaker than that at APP or EGB. One hypothesis for this is that the crop vegetation that dominates at BND and SGP produces far less organic aerosols than the forests around APP and upstream EGB. In addition to a summer scattering peak, BND also exhibited a secondary  $PM_{10}$  and  $PM_1 \sigma_{sp}$  peak during winter months. This was not accompanied by a secondary peak in  $\sigma_{ap}$  (leading to higher  $\omega_0$  during winter) and coincided with lower  $R_{sp}$  and  $R_{ap}$  values and higher  $\alpha_{ap}$  (450/550 nm) values, indicating that larger, primarily scattering particles (including dust) influenced the winter scattering at BND.

Annual  $\omega_0$  cycle amplitudes were substantial at all sites, ranging from  $\sim 0.04$  for  $PM_{10}$  at SGP (February vs. October) to  $\sim 0.13$  for  $PM_1$  at EGB (July vs. October) (Fig. 1). The annual  $PM_{10}$  and  $PM_1 \omega_0$  cycle amplitudes at APP ( $\sim 0.06$ ) appear to be influenced almost entirely by the cycle in  $\sigma_{sp}$ , which in turn was likely influenced by biogenic SOA in the SE US during warm-season months. The large seasonal variability in  $PM_1 \omega_0$  at EGB was due to the variety of  $PM_1$  aerosol sources measured at the site, ranging from very clean air dominated by organics for north and westerly flow to episodic SE flow containing anthropogenically-influenced air masses with high levels of sulfates, organics, and BC (Chan et al., 2010). The low monthly median  $\omega_0$  values at EGB in September and October were more the result of very low aerosol loading

**A multi-year study of lower tropospheric aerosol variability and systematic relationships**

J. P. Sherman et al.

Title Page

Abstract

Introduction

Conclusions

References

Tables

Figures

◀

▶

◀

▶

Back

Close

Full Screen / Esc

Printer-friendly Version

Interactive Discussion

during those months (Fig. 1). Episodic agricultural burning occurs near EGB during fall months, but it is not expected to exert a major influence on median values. Aerosols measured at all sites exhibited a tendency toward lower  $\omega_0$  under clean air conditions for all seasons (as will be discussed in Sect. 3.4.1). Decreases in median  $\omega_0$  at SGP and BND for fall months, relative to summer months, were likely due to a combination of sharp autumn decreases in  $\sigma_{sp}$ , along with increased crop and grass fires and diesel emissions from combines and the transport of crops during the fall harvest. The winter increase in median  $\omega_0$  at BND resulted from the increase in larger, scattering particles during winter, as discussed above.

All sites demonstrated lower median  $b$  values for months and seasons when scattering was highest (most notably summer) and higher  $b$  values when scattering was lowest (autumn months). This relationship was most obvious at APP, where the summer-to-autumn increase in monthly median  $b$  was  $\sim 35\%$ , coinciding with a decrease in median  $\sigma_{sp}$  by a factor of  $\sim 2.5$ . Summer-to-autumn differences in  $R_{sp}$  and  $PM_{10}$   $\alpha_{sp}$  at APP were much less than the differences in  $b$ , an effect that is also observed (to a much lesser degree) at SGP and BND.

Using Mie theory, Collaud Coen et al. (2007) conducted simulations to show that hemispheric backscatter fraction  $b$  at 550 nm is most sensitive to particles of diameter  $D_p < 0.3 \mu\text{m}$  (their Fig. 7 and accompanying discussion). Schuster et al. (2006) combined simulations based on Mie theory with volume size distributions and AOD from AERONET to show that extinction Ångström exponent is relatively insensitive to fine mode effective radius for bi-modal aerosol size distributions and is a better indicator of volume fraction of fine mode aerosol. Smaller seasonal variability in  $\alpha_{sp}$  and  $R_{sp}$  observed at APP, along with higher  $R_{sp}$  values (Figs. 1 and 2), is likely due to a higher and less variable fraction of fine-mode aerosol at APP. This will be discussed further in Sect. 3.4.4. The large summer-to-autumn difference in  $b$  (relative to  $\alpha_{sp}$  and  $R_{sp}$ ) at the four sites suggests that the major seasonal changes in the aerosol size distributions may lie in the lower end of the accumulation mode, with shifts toward larger particles in summer and smaller particles in fall. Photochemistry likely played a role in the ob-

**A multi-year study of lower tropospheric aerosol variability and systematic relationships**

J. P. Sherman et al.

Title Page

Abstract

Introduction

Conclusions

References

Tables

Figures

◀

▶

◀

▶

Back

Close

Full Screen / Esc

Printer-friendly Version

Interactive Discussion

served seasonal cycle of  $b$ , especially at APP (Fig. 1). Gas-to-particle conversion onto existing particles is most efficient for the 100–500 nm size range, since this is where most of the aerosol surface area typically lies (Seinfeld and Pandis, 1998). Reduced conversion in fall (when photochemistry and precursor levels are lower) would impact  $b$  more than  $\alpha_{\text{sp}}$  and  $R_{\text{sp}}$ . Substantial fractions of summer SOA mass measured at APP and SGP consists highly-oxidized “aged” aerosol (Link et al., 2014; Fast et al., 2013).

Absorption Ångström exponents for both wavelength pairs (450/550 nm and 450/700 nm) were lowest during summer months for all three sites where spectral absorption measurements were available (Fig. 2). At APP, the monthly median  $\alpha_{\text{ap}}$  values for both wavelength pairs were similar and well below 1 from May through September, which are the months of maximum biogenic VOC emissions and photochemistry in the SE US (Goldstein et al., 2009). Gyawali et al. (2009) performed simulations using Mie theory to show that  $\alpha_{\text{ap}}$  values much less than 1 are possible (their Figs. 8 and 9) when absorbing particles are coated. Clarke et al. (2007) also reported a large number of  $\alpha_{\text{ap}}$  (470/660 nm) values clustered between 0.7–1.1 for pollution plumes during extensive flights over North America as part the of the INTEX/ICARTT experiment in summer 2004, although they did not hypothesize as to the source of the low  $\alpha_{\text{ap}}$  values. Dust also contributed to July light absorption at SGP, as inferred from the lower monthly median  $R_{\text{ap}}$  (Fig. 2), particularly for the shorter wavelength pair (450/550 nm), where dust absorption is stronger. (Bergstrom et al., 2007). In the colder months, the combined values of  $\alpha_{\text{sp}}$  and  $\alpha_{\text{ap}}$  suggest a mix of absorbing aerosol such as black carbon (BC), along with brown carbon and/or dust (e.g., Cazorla et al., 2013) at SGP, BND, and APP. Lower values of  $R_{\text{ap}}$  during winter at BND suggest some contributions by dust to the absorption. The seasonal cycle of  $\alpha_{\text{ap}}$  at BND and SGP were not as strong as at APP and the elevated winter monthly  $\alpha_{\text{ap}}$  values at APP (in combination with low amounts of super-1  $\mu\text{m}$  aerosol) are consistent with higher winter mass concentrations of SOA from biomass-burning (Link et al., 2014). Wood is a common residential heating fuel in the SE US (Zhang et al., 2010).

## A multi-year study of lower tropospheric aerosol variability and systematic relationships

J. P. Sherman et al.

Title Page

Abstract

Introduction

Conclusions

References

Tables

Figures

◀

▶

◀

▶

Back

Close

Full Screen / Esc

Printer-friendly Version

Interactive Discussion



Median  $PM_{10}$  DRFE at EGB was the least negative of all sites for nearly all months, for reasons that are not obvious based solely on examination of the seasonality in median  $\omega_0$  and  $b$  (relative to that of the other sites). The  $PM_{10}$  and  $PM_{10}$  DRFE cycle amplitudes were generally only a few percent at all sites, with the exception of  $PM_{10}$  DRFE at EGB (and to a lesser degree BND) in early fall. The lack of seasonality (more so at APP and SGP) was due to the competing effects of changes in  $\omega_0$  and  $b$  at the sites for most months. Months with higher aerosol loading (e.g., summer months) coincided with larger, less absorbing particles (lower  $b$  and higher  $\omega_0$ ) at all sites and months with lower loading, such as most autumn months, coincided with smaller, more absorbing particles (higher  $b$  and lower  $\omega_0$ ). These results are in agreement with systematic relationships between  $b$ ,  $\omega_0$ , and aerosol loading, presented in Sects. 3.4.1 and 3.4.2. Lower  $\omega_0$  likely contributed to less negative median  $PM_{10}$  DRFE at EGB and BND during autumn, in spite of higher  $b$  values.

### 3.1.3 Influence of time period studied on annual cycles of aerosol properties at SGP and BND

Inter-annual variability studies require a longer dataset than currently available at EGB and APP, so this topic must wait for a future publication. However, changes in the annual cycle of median aerosol properties and the influence of length of dataset can be studied in a simple manner for SGP and BND, which both have measurements beginning in the mid-1990s. Here we present a comparison of the annual cycles for three time periods: (1) the 1997–2000 period at SGP and 1996–2000 period at BND, coinciding with the period studied by D&O2002, (2) the 2010–2013 period of the current study; and (3) the long-term record (1997–2013 for SGP and 1996–2013 for BND) containing both studies and the period in between.

Median  $PM_{10}$  ( $PM_{10}$ )  $\sigma_{sp}$  for the 2010–2013 period was only  $\sim 75\%$  ( $\sim 65$  to  $70\%$ ) that of the D&O2002 period and  $\sim 90\%$  ( $\sim 85\%$ ) of the median value for the long-term period at both sites, as seen from the “ALL” values in Fig. 3. The decreases in  $PM_{10}$  and  $PM_{10}$  scattering at both sites for the current period were fairly constant

**A multi-year study of lower tropospheric aerosol variability and systematic relationships**

J. P. Sherman et al.

Title Page

Abstract

Introduction

Conclusions

References

Tables

Figures

◀

▶

◀

▶

Back

Close

Full Screen / Esc

Printer-friendly Version

Interactive Discussion

across the seasons, although differences between current period and D&O2002 for a few individual months (February at SGP and October at BND) were larger. The larger reductions in  $PM_{10}$   $\sigma_{sp}$  led to lower  $R_{sp}$  values for all months of the current period, relative to D&O2002 (Fig. 3), although the seasonality in  $R_{sp}$  was similar for the three periods at both sites. The difference between current period and long-term  $R_{sp}$  was larger than the difference between long-term and D&O period  $R_{sp}$  for all months at both sites, indicating that much of the reduction in the influence of  $PM_{10}$  to total aerosol light scattering may have occurred during the current period. The substantial decrease in  $\sigma_{sp}$  at both sites is consistent with other studies (Collaud Coen et al., 2013; Hand et al., 2014) that presented large decreases in surface light scattering and light extinction in North America during the past decade.

Median  $PM_{10}$  and  $PM_{10}$  absorption ( $\sigma_{ap}$ ) for the current period at BND was noticeably lower than for the 1996–2000 period (i.e. the D&O2002 period) for most months, with the most notable reductions occurring during April, September, and October (Fig. 3). These could be the result of decreases in the frequency of agricultural burning that impact the site during spring and fall (D&O2002). The slightly lower absorption measured by the CLAP, relative to the PSAP (Sect. 2.2), may also have played a minor role in the lower median absorption measured during the current period at BND. Median  $PM_{10}$  and  $PM_{10}$   $\omega_0$  values at BND showed little change among the three periods for individual months, and for the periods as a whole. Both  $PM_{10}$  and  $PM_{10}$  absorption at SGP changed less than scattering among periods, resulting in lower median  $\omega_0$  values for most months of the current period, and for the period as a whole. This could suggest that the major sources of scattering and absorbing particles at BND are similar now to those in 1996–2000, while at SGP there may be new sources for absorbing particles (e.g., increased gas/oil production). Collaud Coen et al. (2013) did not analyze the SGP absorption data for trends, but they reported a decreasing trend in absorption at BND consistent with the observations here. While trend analyses of derived aerosol properties such as  $\omega_0$  would provide a valuable expansion of the analysis conducted by Collaud Coen et al. (2013), by providing information on processes affecting the aerosol

characteristics over time, such an analysis is beyond the scope of the current paper and will form the subject of a future publication.

In addition to the decreases in  $R_{sp}$  at SGP and BND for the current period, there were also differences in other indicators of aerosol size distribution between the periods. The median  $PM_1$   $b$  at both sites for the current period was  $\sim 20\%$  higher than for the D&O2002 period and monthly median  $b$  was higher for all individual months of the current period. Median  $PM_{10}$  and  $PM_1$   $b$  values for the current period were also higher than the long-term period values for all months at BND and most months at SGP. This indicates shifts in the lower size region of the accumulation mode (e.g., particles with  $D_p \sim 0.1\text{--}0.3\ \mu\text{m}$ ) toward smaller particles over all seasons at both sites, based on similar reasoning to that of the previous section. Scattering Angstrom exponent ( $\alpha_{sp}$ ) at SGP was lower by small amounts ( $\sim 0.1\text{--}0.3$ ) for all months of the current period, relative to D&O2002 (D&O2002 had very similar annual cycle to long-term period), which is consistent with the observed decrease in  $R_{sp}$  and suggests increasing relative contributions to scattering by coarse mode particles at SGP. In contrast, the amplitude of the annual cycle of median  $\alpha_{sp}$  at BND has changed very little, despite the decrease in  $R_{sp}$  at that site. The likely cause is different shifts in the size distributions at the two sites. One possible source for reduction in  $PM_1$  scattering at BND could be reduced emissions of anthropogenic precursor gases (mainly  $SO_2$ ) by power plants in the region. BND is located in one of the US regions with highest sulfate burdens during the D&O2002 period (Koloutsou-Vakakis et al., 2001). Annual US  $SO_2$  emissions from power plants decreased at a rate of  $\sim 6\% \text{ year}^{-1}$  from 2001–2010, corresponding to the period in between to the D&O2002 study to the beginning of our study, with similar reductions in sulfate concentrations at rural US sites (Hand et al., 2012). Reduced gas-to-particle conversion resulting from reductions in gas-phase precursor emissions would shift the lower size region of the accumulation mode toward smaller particles and thereby reduce  $PM_1$  scattering, while leaving the larger region of the size distribution less affected. The shift in size distribution at SGP also appears to be toward smaller aerosols in the lower size region of accumulation mode (as suggested by larger  $b$ ) but

## A multi-year study of lower tropospheric aerosol variability and systematic relationships

J. P. Sherman et al.

Title Page

Abstract

Introduction

Conclusions

References

Tables

Figures

◀

▶

◀

▶

Back

Close

Full Screen / Esc

Printer-friendly Version

Interactive Discussion



## A multi-year study of lower tropospheric aerosol variability and systematic relationships

J. P. Sherman et al.

Title Page

Abstract

Introduction

Conclusions

References

Tables

Figures

◀

▶

◀

▶

Back

Close

Full Screen / Esc

Printer-friendly Version

Interactive Discussion



with a larger relative contribution from coarse-mode aerosols (as evidenced by smaller  $R_{sp}$  and  $\alpha_{sp}$ ). The source for this shift in size distribution could be less gas-to-particle conversion, along with a new source of large particle aerosol (fracking or oil production in the region or else dust associated with more pronounced droughts during recent years. The annual cycle in median  $PM_{10}$  and  $PM_1$  absorption Ångström exponent ( $\alpha_{ap}$ ) changed very little at BND and SGP, although  $\alpha_{ap}$  measurements at these sites were only initiated in the mid-2000s. Likewise, the changes in the annual cycle of  $PM_{10}$  and  $PM_1$  DRFE were small at both sites, although small decreases (more negative values) were observed at BND for all months.

### 3.2 Weekly cycle of aerosol extensive and intensive properties

Hourly-averaged aerosol properties were binned by day of week over the 2010–2013 period to examine their weekly cycles and to compare the weekly cycles across periods at the long-term sites (SGP and BND), in a similar manner to the annual cycle analysis of Sect. 3.1. Day of week variability in aerosol properties can be used as a tool for distinguishing anthropogenic from natural aerosol sources, since natural sources would not be expected to have aerosol properties that vary on weekly scales (Murphy et al., 2008). Due to the dependence of most aerosol properties on season (Sect. 3.1.2), the weekly cycles in the current period were examined over full years and also for individual seasons.

#### 3.2.1 Day of week variability as a function of region

There was small day of week variability in median scattering and all intensive properties for all sites over the 2010–2013 period, with larger variability in absorption. The amplitudes of the weekly  $PM_{10}$  and  $PM_1$   $\sigma_{sp}$  cycles were  $\sim 10\%$  or less at all sites, when examined over full years (Fig. S2 in the Supplement to this paper). The weekly  $\sigma_{sp}$  cycle amplitudes were also  $10\%$  or less for all individual seasons at EGB and for all seasons except autumn at BND, when it was roughly  $30\%$ , with maxima on Tuesday

## A multi-year study of lower tropospheric aerosol variability and systematic relationships

J. P. Sherman et al.

Title Page

Abstract

Introduction

Conclusions

References

Tables

Figures

◀

▶

◀

▶

Back

Close

Full Screen / Esc

Printer-friendly Version

Interactive Discussion

and Wednesday. It reached 20 % during fall and winter at SGP (with a mid-week peak during autumn and no real pattern during winter). Median  $PM_{10}$  and  $PM_1$   $\sigma_{sp}$  during summer at APP was constant for Sunday–Tuesday, followed by a  $\sim 25$  % step increase on Wednesday, after which it decreased at a very slow rate through Saturday. A similar but less pronounced weekly  $\sigma_{sp}$  cycle was present in spring at APP and absorption followed a similar weekly cycle at APP for all seasons except winter, as discussed below. Link et al. (2014) analyzed the relative abundances of light hydrocarbons to alkyl nitrates measured at APP, and concluded from alkyl nitrate formation kinetics that most of the air masses measured during the sampling period had undergone one to three days of photochemical processing. The step-like increase in  $\sigma_{sp}$  on Wednesday and higher values through Saturday is thus consistent with regional emissions during Monday–Friday. The fact that this occurs primarily during the warm season could be due to convectionally-driven increases in regional transport.

The amplitude of the weekly cycle in median  $b$  and  $\omega_0$  for both size cuts was  $\sim 0.01$  or less at all sites for all seasons, with the exception of summer and fall  $PM_1$   $\omega_0$  at EGB, where it was 0.02 in summer (lowest on Friday) and 0.03 in fall (lowest on Tuesday). The amplitudes of the aerosol scattering and absorption Ångström exponent ( $\alpha_{sp}$  and  $\alpha_{ap}$ ) cycles were on the order of 0.1 or less for all seasons at all sites. Day of week median DRFE fluctuated by  $\sim 1 W m^{-2}$  or less except for  $PM_1$  DRFE at EGB, which had variability of between 2 and  $3 W m^{-2}$  for all seasons, with most negative values on Sundays and least negative on Tuesday and Wednesdays (Fridays in summer). Day of week median  $R_{sp}$  and  $R_{ap}$  variability was negligible for all seasons at APP ( $\sim 0.01$ ), small at BND ( $\sim 0.03$ ), and slightly larger ( $\sim 0.05$ ) at SGP. The minimum median  $R_{sp}$  at SGP occurred on Tuesday for all seasons, possibly due to some weekly pattern in agricultural activity near the site.

The amplitudes of the weekly cycles in median  $\sigma_{ap}$  over full years (the “All Months” plot in Fig. 6) were higher ( $\sim 15$ – $30$  %) than those in  $\sigma_{sp}$  at all sites and were highest for APP and EGB. Median absorption at all sites was lowest on Sunday and/or Monday when studied over full years. The apparently lower Sunday and Monday  $\sigma_{ap}$  at SGP

(Fig. 6) was possibly an artifact due to the lack of PSAP filter changes on weekends at the site; weekend days with high absorption would lead to overloaded filters and under-representation in the database, while weekend days with low absorption would be well-represented. Figure 6 also shows the weekly cycle of median  $\sigma_{ap}$  for individual seasons, which reveal several features not seen on the annual plot, namely (1) the absorption minima on Sunday and Monday was observed at APP (and possibly SGP) over all individual seasons but was not observed at BND during fall and winter or at EGB during spring, (2) weekly cycle amplitude in median  $\sigma_{ap}$  was often significantly larger (up to  $\sim 60\text{--}70\%$  for SGP and EGB) for individual seasons (Fig. 6), (3) the weekly absorption cycle at APP followed the same general progression for all seasons except winter, with steady increases leading to a broad maximum on Wednesday–Friday, followed by a weekend decrease. The cycle amplitude was largest in summer, similar to that of scattering at APP. The discussions above related to summer weekly scattering cycle at APP may also apply for the absorption cycle at APP, (4) BND exhibits strong day of week  $\sigma_{ap}$  variability during all seasons except winter (when convection and transport is weakest) but the peak day varies with season. Median  $\sigma_{ap}$  at BND exhibits a steady increase throughout the week during summer, reaching a peak on Friday, while in autumn the absorption peaks on Tuesday and decreases through the remainder of the week. The summer pattern at BND could be due to convectionally-driven increases in regional transport, with weekly patterns in agricultural and transportation activities the likely source for large cycles during the other seasons. Each of these features illustrates the need to quantify day of week absorption variability on a seasonal basis.

Murphy et al. (2008) utilized speciated mass concentration data from IMPROVE monitoring sites in the US over the years 2000–2006 to study day of week variability in aerosol composition. Results from their study included black carbon and soil dust concentration minima on Sunday and Monday, but minimal weekly cycling of organic carbon or sulfate. One of their conclusions was that diesel emissions likely play a large role in black carbon aerosols over the entire US and that much of the soil dust in the US was likely anthropogenic. They also found that aerosol light absorption at SGP (1999–

## A multi-year study of lower tropospheric aerosol variability and systematic relationships

J. P. Sherman et al.

Title Page

Abstract

Introduction

Conclusions

References

Tables

Figures

◀

▶

◀

▶

Back

Close

Full Screen / Esc

Printer-friendly Version

Interactive Discussion

## A multi-year study of lower tropospheric aerosol variability and systematic relationships

J. P. Sherman et al.

Title Page

Abstract

Introduction

Conclusions

References

Tables

Figures

◀

▶

◀

▶

Back

Close

Full Screen / Esc

Printer-friendly Version

Interactive Discussion

2005) and BND (1999–2002) followed a similar weekly cycle as black carbon and soil dust, while scattering variability on this timescale was negligible. The general lack of weekly scattering variability for all sites in our study and for SGP and BND in other studies (Murphy et al., 2008; Sheridan et al., 2001) could be related to the absence of weekly cycles in organic carbon or sulfate concentrations (Murphy et al., 2008), since these represent the primary sources of PM<sub>1</sub> scattering particles at all sites in our study (Fast et al., 2013; Koloutsou-Vakakis et al., 2001; Chan et al., 2010; Fig. S1 of Supplement to this paper). The larger weekly absorption cycle at all sites (relative to scattering) suggests that the some of the sources for scattering and absorbing aerosols were likely different. The Sunday and Monday  $\sigma_{\text{ap}}$  minima present in nearly all cases of our study and similar weekly variability in  $\sigma_{\text{ap}}$  to that noted by Murphy for BC concentrations in the US (up to  $\sim 20\%$ ) could indicate that diesel emissions played a large role in the absorption measured at each site. The weekly pattern in  $\sigma_{\text{ap}}$  at APP over all seasons except winter indicates that the emissions controlling the weekly absorption cycle were likely regional in nature, as discussed above. This could also be the case for the other sites, although it is not as apparent from Fig. 6.

### 3.2.2 Influence of time period studied on weekly cycles of aerosol properties at SGP and BND

The weekly cycle in median PM<sub>10</sub> and PM<sub>1</sub> aerosol intensive properties exhibited the same lack of variability for the D&O2002 and the long-term periods at SGP and BND as for the current period. The only notable difference in the weekly cycle of aerosol properties between periods was the elevated median PM<sub>10</sub> and PM<sub>1</sub>  $\sigma_{\text{sp}}$  at BND (and to a lesser degree, SGP) on weekends during the D&O2002 period. Amplitudes of the weekly cycle of median PM<sub>10</sub> and PM<sub>1</sub>  $\sigma_{\text{sp}}$  at BND were only  $\sim 10\%$  for full years during the current period (with a broad peak between Tuesday and Thursday) and were even less for the long-term period. However, there was a weekend peak in median PM<sub>10</sub> and PM<sub>1</sub>  $\sigma_{\text{sp}}$  at BND during the D&O2002 period, with values  $\sim 25\%$  higher than for the Wednesday/Thursday minima. A similar weekend peak was observed at SGP during

the D&O2002 period, although it was less pronounced ( $\sim 15\%$  above the Thursday  $\sigma_{sp}$  minima) than at BND. The median  $R_{sp}$  during that period was  $\sim 0.85$  to  $0.90$  for weekend days at both sites during the D&O time period so the enhanced weekend  $\sigma_{sp}$  was likely not dust but rather some anthropogenic  $PM_1$  source that no longer exerts a major influence on  $\sigma_{sp}$ , since the weekend  $\sigma_{sp}$  enhancement is not seen in either the long-term or current period weekly cycle at either site.

### 3.3 Diurnal cycle of aerosol extensive and intensive properties

Hourly-averaged aerosol properties were binned by hour of day over the 2010–2013 period to examine their diurnal cycles and also to compare the diurnal cycles across periods at the long-term sites (SGP and BND), in a similar manner to the weekly cycle analysis of Sect. 3.2. Diurnal variability can be used to infer the influence of local sources and boundary layer height on the dried near-surface aerosol properties, among other things. A purely boundary layer effect at the four non-urban sites would likely give rise to a single broad afternoon minima and late evening to early morning maxima in the diurnal  $\sigma_{sp}$  and  $\sigma_{ap}$  cycles due to the diurnal evolution of the mixed layer height, which is influenced by solar heating. A local traffic influence would result in a diurnal  $\sigma_{ap}$  cycle nearly in phase with local traffic patterns, with peaks typically occurring during early morning and late afternoon to early evening. A local traffic influence would also result in a larger diurnal cycle in  $\sigma_{ap}$  than  $\sigma_{sp}$  for mid-visible wavelengths, due to the higher BC fractions in fresh diesel emissions (US EPA, 2002). Regional traffic sources such as steady interstate traffic can be difficult to separate from boundary layer effects through diurnal cycle timing alone but may be separable based on the relative cycle amplitudes of absorption and scattering. Due to the dependence of most aerosol properties on season (Sect. 3.1.2), the diurnal cycles for the current period were examined over the full year and also for individual seasons.

## A multi-year study of lower tropospheric aerosol variability and systematic relationships

J. P. Sherman et al.

Title Page

Abstract

Introduction

Conclusions

References

Tables

Figures

◀

▶

◀

▶

Back

Close

Full Screen / Esc

Printer-friendly Version

Interactive Discussion



### 3.3.1 Diurnal variability as a function of region

Similar to the weekly cycles, the scattering diurnal cycle amplitudes were modest. When studied over full years, the amplitude of the  $PM_{10}$   $\sigma_{sp}$  diurnal cycle was  $\sim 10\%$  at APP and marginally higher at BND and SGP, with slightly less diurnal variability in median  $PM_1$   $\sigma_{sp}$  at all sites (Fig. 7). Broad mid to late-afternoon  $PM_{10}$  and  $PM_1$   $\sigma_{sp}$  minima were observed at SGB, BND, and ( $PM_1$  only) EGB, consistent with some influence of boundary layer height on the diurnal  $\sigma_{sp}$  cycles. A smaller, narrow early afternoon  $\sigma_{sp}$  minima was observed near 13:00 Local Standard Time (LST) at APP, likely due to a combination of less mid-day local traffic and dilution due to elevated boundary layer heights, the latter of which are derived from vertical aerosol backscatter profiles measured by a micro-pulsed lidar at APP (not shown). The amplitudes of the diurnal cycles in  $PM_{10}$  and  $PM_1$   $\sigma_{ap}$  were larger than those of  $\sigma_{sp}$  at all sites; roughly 30–35% at SGP and BND and  $\sim 15$ –20% at APP and ( $PM_1$  only) EGB (Fig. 7). The larger cycles in  $\sigma_{ap}$  indicate some local and/or regional traffic influence at all sites.

The impact of local traffic on the diurnal  $\sigma_{ap}$  cycle was most notable at APP and EGB, as seen by relatively narrow morning peaks during hours of maximum traffic (07:00–09:00 LST). The afternoon  $\sigma_{ap}$  minima at APP was also narrower than that of the other sites and occurred earlier in the afternoon (near 12:00 LST), similar to the narrow mid-day  $\sigma_{sp}$  minima. The APP site is not located near any major highways but is located 1 to 3 km from local commuter traffic sources during weekday mornings and late afternoons. EGB is a remote site but is located approximately 15 km from a major interstate highway and also experiences some influence from the nearby city Barrie when the wind comes from that direction. The highway experiences heavy commuter traffic during early morning and late afternoon.

SGP and BND demonstrated only a single broad afternoon  $\sigma_{ap}$  minima and broad evening to early morning peak (Fig. 7), suggesting a greater influence of boundary layer height evolution to the  $\sigma_{ap}$  diurnal cycles at these sites, along with possibly regional traffic. Both sites experience infrequent local traffic but are situated  $\sim 8$  to 15 km to

## A multi-year study of lower tropospheric aerosol variability and systematic relationships

J. P. Sherman et al.

Title Page

Abstract

Introduction

Conclusions

References

Tables

Figures

◀

▶

◀

▶

Back

Close

Full Screen / Esc

Printer-friendly Version

Interactive Discussion



## A multi-year study of lower tropospheric aerosol variability and systematic relationships

J. P. Sherman et al.

Title Page

Abstract

Introduction

Conclusions

References

Tables

Figures

◀

▶

◀

▶

Back

Close

Full Screen / Esc

Printer-friendly Version

Interactive Discussion

the west (and predominantly upwind) of major interstate highways (I-35 for SGP and I-57 for BND) that experience truck traffic over all hours, with some increase in traffic volume during early morning. Thus regional traffic may have contributed to the diurnal cycles in  $\sigma_{ap}$  (and to a lesser extent  $\sigma_{sp}$ ) at SGP and BND, in contrast to the commuter influence at APP and the mixture of regional and commuter traffic influence at EGB.

Diurnal variability of aerosol intensive properties was minimal at all sites when studied over full annual cycles, with a few minor exceptions: (1) a small early morning decrease ( $\sim 0.05$ ) in  $R_{ap}$  at SGP, (2) small (0.2) decreases in  $\alpha_{ap}$  (450/550 nm) during the day at BND, SGP, and a smaller amount at APP during the day, possibly indicative of a greater relative influence of BC to the absorption.

The diurnal variability of  $\sigma_{ap}$  was much larger than the day of week variability for all individual seasons at SGP and BND, winter and spring at APP, and summer and fall at EGB (Fig. 8). The amplitude of the diurnal  $PM_{10}$  and  $PM_1$   $\sigma_{ap}$  cycles at APP were  $\sim 15$ – $20$  % for all seasons and were  $\sim 40$  % for all seasons at SGP. Features similar to those over full annual cycles were present for each individual season at APP and SGP, namely the influence of morning commuter traffic at APP and the broad single peak and minima suggesting boundary layer influence and possibly regional traffic at SGP. In contrast, the amplitude of the diurnal  $\sigma_{ap}$  cycles at BND and EGB varied substantially with season and was largest in summer and fall at both sites. The seasonally-dependent diurnal  $\sigma_{ap}$  cycle amplitudes at BND (Fig. 8), along with the widths of the single broad daytime minima and night-time maxima that coincided with the diurnal cycle of solar insolation for all seasons, seem to implicate boundary layer dynamics for at least part of the large diurnal  $\sigma_{ap}$  cycle. The large summer and fall  $PM_1$   $\sigma_{ap}$  diurnal cycles at EGB showed some influence from boundary layer height (e.g., the broad late morning to afternoon minima and the late evening maxima), in addition to the local traffic influence observed during autumn mornings. However, the summer and fall  $\sigma_{ap}$  diurnal cycles at EGB also include a peak within two hours of local midnight, followed by sharp decreases until  $\sim 05:00$  LST. This is not consistent with known traffic patterns near the site nor with a boundary layer height influence. One

other interesting feature in the  $\sigma_{ap}$  cycles is that the time of morning peak at APP and EGB lags the time of the peak at BND and SGP by roughly two hours for all seasons. Possible explanations include (1) differences in morning boundary layer heights over cropland and forested areas; and (2) differences in traffic sources (as discussed in the previous paragraphs).

The diurnal cycle amplitudes of most aerosol intensive properties were small for all seasons, as illustrated in Figs. S3–S6 of the Supplement. The amplitudes of the  $PM_{10}$  and  $PM_1$   $b$  cycles were  $\sim 0.01$  or less at all sites for all seasons and the  $\alpha_{sp}$  cycle amplitudes were  $\sim 0.1$  or less for all sites and seasons, with exception of summer at SGP (when it was 0.3, with minima near hour 18:00 LST). Diurnal variability of  $R_{sp}$  was negligible for APP and was  $\sim 0.03$  for SGP and BND for all seasons except summer at BND, where it was  $\sim 0.05$  (with minima near 06:00 LST). These small cycle amplitudes are comparable to those for the weekly cycles and indicate that median values of indicators of aerosol size distributions at all sites exhibited little variability on shorter time scales (diurnal and day of week).

The amplitude of the diurnal  $R_{ap}$  cycle was only  $\sim 0.02$  for all seasons at BND and APP but was larger at SGP, with morning minima in  $R_{ap}$  at SGP coinciding with hours of peak traffic (07:00 to 10:00 LST). The morning minima in  $R_{ap}$  at SGP are most obvious in summer, with values  $\sim 0.10$  less than the daily maxima. In addition, the hour of minimum  $R_{ap}$  for all seasons coincided with times of low absorption, signifying lower levels of absorbing  $PM_1$  during this time as opposed to elevated levels of absorbing mineral dust generated by agricultural activities or traffic near the site.

Diurnal variability in median  $PM_{10}$  and  $PM_1$   $\omega_0$  was slightly larger than day of week variability but much less than seasonal variability at all sites, with cycle amplitudes of  $\sim 0.01$  to 0.02 for most sites and seasons. There were a few exceptions. The  $PM_1$   $\omega_0$  diurnal cycle amplitude at SGP was  $\sim 0.03$  during summer and  $\sim 0.04$  in fall, with broad afternoon maxima and late evening to early morning minima for both seasons, influenced by the  $\sigma_{ap}$  diurnal cycle. Diurnal variability in  $PM_1$   $\omega_0$  at EGB was  $\sim 0.04$  during summer (with the same broad afternoon peak and late evening to early morn-

## A multi-year study of lower tropospheric aerosol variability and systematic relationships

J. P. Sherman et al.

Title Page

Abstract

Introduction

Conclusions

References

Tables

Figures

◀

▶

◀

▶

Back

Close

Full Screen / Esc

Printer-friendly Version

Interactive Discussion



## A multi-year study of lower tropospheric aerosol variability and systematic relationships

J. P. Sherman et al.

Title Page

Abstract

Introduction

Conclusions

References

Tables

Figures

◀

▶

◀

▶

Back

Close

Full Screen / Esc

Printer-friendly Version

Interactive Discussion

ing minima as SGP) and was  $\sim 0.05$  in fall (with sharp minima near 07:00 LST and 19:00 LST likely due to local traffic). The variability in  $\omega_0$  at EGB led to diurnal variability in DRFE of  $3 \text{ W m}^{-2}$  in summer and  $4 \text{ W m}^{-2}$  in fall. Diurnal variability in median DRFE was typically 1 to  $2 \text{ W m}^{-2}$  for all other sites and seasons. Diurnal variability in median  $\alpha_{\text{ap}}$  (450/700 nm) was negligible for SGP, BND, and APP for all individual seasons but there were small cycles in  $\alpha_{\text{ap}}$  (450/550 nm) of  $\sim 0.2$  at BND during all seasons, SGP during winter and spring, and APP during summer, with smaller cycles during the other seasons. In all cases, the highest median  $\alpha_{\text{ap}}$  (450/550 nm) values occurred over the early evening hours until near sunrise, with minima during early to mid-morning at SGP and BND and afternoon at APP. Increases in absorption in the blue-violet portion of visible spectrum are indicative of non-BC sources (dust or brown carbon). No consistent patterns in the diurnal cycles in median  $R_{\text{sp}}$  and  $R_{\text{ap}}$  were present to indicate the influence of dust to the small cycle of  $\alpha_{\text{ap}}$  (450/550 nm) and biomass burning influences the three sites to various degrees during the year so it is possible that brown carbon produced by wood burning could be responsible for the small diurnal cycles in  $\alpha_{\text{ap}}$  (450/550 nm).

### 3.3.2 Influence of time period studied on diurnal cycles of aerosol properties at SGP and BND

Median  $\text{PM}_{10}$  and  $\text{PM}_1$   $\sigma_{\text{sp}}$  and  $\sigma_{\text{ap}}$  at BND were lowest for all hours of the most recent (2010–2013) period, as was the diurnal cycle amplitude of each parameter (Fig. 7). Median  $\sigma_{\text{sp}}$  at SGP was also lowest for this period over all hours and the diurnal variability was perhaps slightly less than for the other two periods (1997–2000 and 1997–2013). The amplitude of the diurnal cycle in median  $\sigma_{\text{ap}}$  at SGP was slightly larger for the most recent period, with a more pronounced absorption dip from late morning through early evening. This gave rise to a larger cycle amplitude in median  $\omega_0$  at SGP for the most recent period ( $\sim 0.03$  for  $\text{PM}_1$  and  $0.02$  for  $\text{PM}_{10}$ ) than for either the D&O2002 or long-term periods ( $\sim 0.01$  for both periods). In addition there was a slightly larger DRFE variability ( $\sim 2 \text{ W m}^{-2}$ ) for the most recent period. Diurnal cycle amplitude in

## A multi-year study of lower tropospheric aerosol variability and systematic relationships

J. P. Sherman et al.

Title Page

Abstract

Introduction

Conclusions

References

Tables

Figures

◀

▶

◀

▶

Back

Close

Full Screen / Esc

Printer-friendly Version

Interactive Discussion

median  $\omega_0$  at BND was small ( $\sim 0.01$ ) for all three periods, as was that of DRFE variability ( $\sim 1 \text{ W m}^{-2}$ ). The results for all indicators of aerosol size were similar to those in Sect. 3.1.3, with highest median  $b$  and lowest median  $R_{\text{sp}}$  occurring during the 2010–2013 period for all hours at both sites, along with negligible inter-period changes in median  $\alpha_{\text{sp}}$  for all hours at BND. Median values of  $\alpha_{\text{sp}}$  at SGP were slightly lower (by  $\sim 0.1$ – $0.2$ ) for all hours of the most recent period. There was small diurnal variability for each of these properties over any period at either site, signifying that the aerosol size distributions likely exhibited little diurnal variability over any of the periods.

### 3.4 Systematic relationships among aerosol properties

Systematic relationships among aerosol intensive properties and aerosol loading were explored at the four North American sites for the 2010–2013 period, both on an annual basis and broken down by season (Figs. 9–12). D&O2002 suggested systematic relationships would be useful for constraining model parameterization of aerosol optical properties and for reducing uncertainties in satellite-based retrievals of aerosol optical depth, which make assumptions regarding aerosol size distributions and  $\omega_0$  (Levy et al., 2010). Systematic relationships can also provide information regarding aerosol source types and processes. Relationships between mean aerosol intensive properties and aerosol loading, represented by aerosol light scattering  $\sigma_{\text{sp}}$  at 550 nm, were investigated for each season at each site by separating hourly-averaged  $\sigma_{\text{sp}}$  values into  $10 \text{ M m}^{-1}$  bins and then calculating the mean aerosol optical properties for each  $\sigma_{\text{sp}}$  bin. The  $x$  values for the data points on each plot correspond to the bin center. The relatively high  $\omega_0$  values at all sites justifies the use of  $\sigma_{\text{sp}}$  as a proxy for loading. Mean values were used to facilitate comparisons with D&O2002. Similar to the methods in Andrews et al. (2011), the standard error (SE = SD/square root of number of sample points) of the aerosol property was calculated for each  $\sigma_{\text{sp}}$  bin, and the bin was only included on the systematic variability plot if the standard error was less than 5 % of the typical  $y$  axis parameter value. These standard error thresholds were set at the follow-

ing:  $\omega_0$ : 0.05,  $b$ : 0.005, DRFE: 1,  $\alpha_{ap}$ : 0.05,  $\alpha_{sp}$ : 0.1,  $R_{sp}$ : 0.037. For brevity, only the  $PM_{10}$  curves are shown for SGP, BND, and APP, along with  $PM_1$  curves for EGB. The corresponding  $PM_1$  curves at SGP, BND, and APP look similar to the  $PM_{10}$  curves for these sites. Relationships between a few select intensive properties are also included to provide more insight into aerosol sources and/or processes influencing the properties measured at the sites. The same 5% SE thresholds for the dependent variable were also applied to these plots.

### 3.4.1 Single scattering albedo and backscatter fraction vs. scattering coefficient

Single scattering albedo increased and hemispheric backscatter fraction decreased with increasing aerosol loading for most sites and seasons (Fig. 9), indicative of greater influences by smaller, darker particles under low loading conditions and by larger, brighter particles under high loading conditions. Lower  $\omega_0$  and higher  $b$  values for low aerosol loading have been reported in other studies (D&O2002, Andrews et al., 2011) and are consistent with preferential removal of large, scattering particles by cloud scavenging and/or deposition. They can also be the result of new particle formation with growth by condensation and/or coagulation to optically-active sizes (Andrews et al., 2011).

The relative contributions of scattering and absorption to light extinction remained nearly constant for  $\sigma_{sp}$  greater than  $45 \pm 10 \text{ M m}^{-1}$  for all seasons except spring at EGB, suggesting that primary sources of scattering and absorbing aerosol were responsible for the high loading events at EGB for most seasons- likely pollution transport from the south/southeast. Primary aerosol influence was also seen over most of the  $\sigma_{sp}$  range during spring at SGP and winter at APP. These are seasons with larger biomass burning influence in the two regions, namely field and crop burning during spring at SGP (Kohler et al., 2011) and regional wood-burning in the SE US during colder months (Zhang et al., 2010).

## A multi-year study of lower tropospheric aerosol variability and systematic relationships

J. P. Sherman et al.

Title Page

Abstract

Introduction

Conclusions

References

Tables

Figures

◀

▶

◀

▶

Back

Close

Full Screen / Esc

Printer-friendly Version

Interactive Discussion



## A multi-year study of lower tropospheric aerosol variability and systematic relationships

J. P. Sherman et al.

Title Page

Abstract

Introduction

Conclusions

References

Tables

Figures

◀

▶

◀

▶

Back

Close

Full Screen / Esc

Printer-friendly Version

Interactive Discussion



Regions of the  $\omega_0$  vs.  $\sigma_{sp}$  curves with positive slopes indicate different sources of scattering and absorbing aerosol, with particle growth often leading to the larger relative contributions by scattering. Single-scattering albedo increased with  $\sigma_{sp}$  for all seasons at BND and for all but the above-mentioned seasons at SGP, EGB, and APP. It also increased up to  $\sim 45 \text{ M m}^{-1}$  for all seasons at EGB. The larger, more reflective particles with increased loading at APP during summer (and to a lesser degree spring and fall) may be due to condensation of organic and inorganic matter onto existing particles, as discussed in Sects. 3.1.2 and 3.4.7. Most of the spring and fall high-loading events at APP occur close to summer when emissions and photochemistry are significant. The SGP  $\omega_0$  vs.  $\sigma_{sp}$  curves for most seasons demonstrate a positive slope over a majority of the range of observed loading values, followed by some degree of flattening at high  $\omega_0$  values for  $\sigma_{sp} \geq 55 \text{ M m}^{-1}$ . Similar characteristics are present in the winter curve at BND. Primary sources such as wind-blown dust could have contributed to the large, highly reflective particles influencing high-loading summer and winter events at SGP and winter events at BND, as mean  $R_{sp}$  decreased sharply with increasing  $\sigma_{sp}$  during these seasons (Fig. 11).

### 3.4.2 Direct radiative forcing efficiency vs. scattering coefficient

Unlike  $\omega_0$  and  $b$ , the DRFE vs.  $\sigma_{sp}$  relationship did not follow a distinct trend and was unique to each site (Fig. 9). On an annual basis, DRFE for SGP became slightly less negative with increasing  $\sigma_{sp}$ , similar to that presented in D&O2002. Although the shapes of the SGP curves varied with season, the DRFE values for all but lowest and highest loading were within 2–3% of the annual curve. Similarly, the annual DRFE for APP became slightly less negative with increasing  $\sigma_{sp}$  over a large majority of the curve, with slightly larger slopes for the winter and summer curves and DRFE values lying within 4–5% of the annual curve for all but the lowest loading (where aerosol forcing is less important) over all seasons. The overall small increase in DRFE with increasing  $\sigma_{sp}$  indicates that, in terms of DRFE, the  $b$  vs.  $\sigma_{sp}$  relationship was slightly more important than the  $\omega_0$  vs.  $\sigma_{sp}$  relationship for most seasons and loading levels at







seasonal variability in  $R_{sp}$  (Fig. 2) would then be consistent with the lack of seasonality in  $\alpha_{sp}$  at the sites. The  $\alpha_{sp}$  vs.  $\sigma_{sp}$  curves for  $PM_1$  at EGB were not displayed, due to the difficulty in relating  $PM_1$   $\alpha_{sp}$  to fine mode aerosol fraction.

### 3.4.6 Absorption Ångström exponent vs. scattering Ångström exponent

5 Mean absorption Ångström exponent  $\alpha_{ap}$  (450/700 nm), calculated for scattering Ångström exponent  $\alpha_{sp}$  (450/700 nm) bin sizes of 0.1 are shown for SGP, BND, and APP in Fig. 12. Absorption Ångström exponent decreased with increasing  $\alpha_{sp}$  for all seasons at SGP and BND and during summer at APP and showed little variation with  $\alpha_{sp}$  during the other seasons at APP (Fig. 12). Based on the  $R_{sp}$  vs.  $\alpha_{sp}$  relationships  
10 (Sect. 3.4.4 and Fig. 11), most of the higher values of  $\alpha_{ap}$  at SGP and BND (coinciding with low  $\alpha_{sp}$  values) occurred when there was a larger relative influence by coarse mode aerosol (presumably dust). These occurred during all seasons at SGP, autumn only at BND, and very rarely during any season at APP, as indicated by the number of points in  $\alpha_{sp}$  bins below  $\sim 1.0$  (Fig. 12). Based on this, dust appears to have influenced aerosol absorption the most at SGP for all seasons and likely exerted little influence on the absorption at APP. The contribution to absorption by dust in fall at BND could be the result of airborne dust generated during harvesting season. The larger dust influence at SGP, relative to BND, could be due to (1) generally drier conditions in OK than in IL, (2) more unplanted fields near SGP than near BND, where corn and soybean are planted on most fields. Lower values of  $\alpha_{ap}$  during non-summer months at all sites generally were near 1 and corresponded to higher  $\alpha_{sp}$  values, likely due to an increasing BC contribution to absorption. The higher and nearly constant winter values of  $\alpha_{ap}$  at APP ( $\sim 1.2$ – $1.3$ ) and insensitivity to  $\alpha_{sp}$  (along with high  $R_{sp}$  values) also indicate a likely influence of brown carbon to winter absorption at APP, likely from regional wood-burning.  
25

Summer values of mean  $\alpha_{ap}$  were lower than those of other seasons for all  $\alpha_{sp}$  bins at BND and APP and for all but the lowest  $\alpha_{sp}$  bins at SGP (where dust likely influenced

## A multi-year study of lower tropospheric aerosol variability and systematic relationships

J. P. Sherman et al.

Title Page

Abstract

Introduction

Conclusions

References

Tables

Figures

◀

▶

◀

▶

Back

Close

Full Screen / Esc

Printer-friendly Version

Interactive Discussion

absorption). The slopes of the  $\alpha_{ap}$  vs.  $\alpha_{sp}$  curves indicates that  $\alpha_{ap}$  values below 1 during summer coincided with higher fractions of fine-mode aerosol (higher  $\alpha_{sp}$ ). The curves for individual seasons lie close to the annual curves, with the exceptions of summer at SGP and BND and summer and winter at APP.

### 3.4.7 Absorption Ångström exponent vs. single-scattering albedo

The individual season  $\alpha_{ap}$  vs.  $\omega_0$  relationships (Fig. 12) at SGP, BND, and APP were similar to the annual curves for all seasons except summer. The summer curve at BND was also similar the annual BND curve except at high  $\omega_0$ . Mean  $\alpha_{ap}$  during these seasons remained constant or slightly increased with increasing  $\omega_0$  until  $\omega_0$  approached 0.90 (specifically the  $\omega_0$  bin centered at 0.875), with values near  $1.2 \pm 0.1$ . This was followed by sharp decreases in  $\alpha_{ap}$  with further increases in  $\omega_0$ . Values above 1 during non-summer month lower  $\omega_0$  conditions suggest some contribution from organic carbon and/or dust to the dominant absorption by black carbon (e.g., Cazorla et al., 2013); the  $\alpha_{ap}$  vs.  $\alpha_{sp}$  and  $R_{sp}$  vs.  $\alpha_{sp}$  relationships point to dust for SGP and BND and to brown carbon at APP. This occurred most frequently during the non-summer seasons at APP and least frequently at SGP, based on the number of points in  $\omega_0$  bins below 0.90.

Some of the same qualitative features were present in the summer curves but mean  $\alpha_{ap}$  was lower over the entire  $\omega_0$  range (more so for SGP and APP) and values were well below 1 for  $\omega_0 > 0.90$  at BND and APP. From the  $b$  vs.  $\omega_0$  relationships (Fig. 10), the lower mean  $\alpha_{ap}$  values at all sites during summer also coincided with lower mean  $b$  values. When combined, this indicates that lower mean  $\alpha_{ap}$  values were associated with larger, more reflective fine-mode particles. Gyawali et al. (2009) reported a similar  $\alpha_{ap}$  vs.  $\omega_0$  relationship for summer months without a biomass burning influence in Reno, NV with a near constant  $\alpha_{ap} \sim 1.1$ – $1.2$  up to  $\omega_0 \sim 0.90$ , followed by  $\alpha_{ap}$  values mostly below one for higher  $\omega_0$ . They attributed this wavelength dependence of absorption to particles coated with non-absorbing organic and inorganic matter. It should be noted that they used a photo-acoustic spectrometer (as compared to the filter-based

## A multi-year study of lower tropospheric aerosol variability and systematic relationships

J. P. Sherman et al.

Title Page

Abstract

Introduction

Conclusions

References

Tables

Figures

◀

▶

◀

▶

Back

Close

Full Screen / Esc

Printer-friendly Version

Interactive Discussion



**A multi-year study of lower tropospheric aerosol variability and systematic relationships**

J. P. Sherman et al.

Title Page

Abstract

Introduction

Conclusions

References

Tables

Figures

◀

▶

◀

▶

Back

Close

Full Screen / Esc

Printer-friendly Version

Interactive Discussion

techniques used at the sites in this study) and also used different wavelengths (405 and 870 nm) so the results are not directly comparable. The summer values of  $\alpha_{ap}$  at APP were also much lower for all  $\omega_0$  than those reported by Gyawali et al. (2009). Possible biases in filter-based absorption measurements made in high-organic aerosol environments could in principle also contribute to this result (e.g., Lack et al., 2008, 2009). A detailed analysis of the effects, both real and artifact, of absorbing and non-absorbing coatings on the wavelength-dependence of light absorption by black carbon is beyond the scope of this paper.

**3.4.8 Absorption Ångström exponent vs. scattering coefficient**

When studied on an annual basis, mean  $\alpha_{ap}$  decreased with increasing aerosol loading at SGP, BND, and APP, with the smallest negative slope at SGP and the largest at APP (Fig. 12). For most non-summer seasons (and even summer at SGP) the mean  $\alpha_{ap}$  values at all sites were in the range 0.9–1.2 over much of the  $\sigma_{sp}$  range, indicating that much of the absorption during these seasons was likely due to BC. A noticeable exception is winter at APP, where mean  $\alpha_{ap}$  was independent of  $\sigma_{sp}$  and the value of  $\sim 1.3$  is indicative of either some dust or brown carbon influence. The high and relatively constant  $R_{sp} \sim 0.85$  seems to point to brown carbon, possibly from local and/or regional wood-burning during winter. In contrast, summer  $\alpha_{ap}$  at BND and APP was much more sensitive to loading, in addition to possessing much lower mean  $\alpha_{ap}$  values for all levels of loading than during other seasons. Mean summer  $\alpha_{ap}$  values were well under 1 for all but the lowest loading conditions at both sites (especially APP), possibly influenced by condensation of organic and/or inorganic material on absorbing cores, as discussed in the previous section.

## 4 Summary and conclusions

Seasonal variability in scattering, absorption, and most aerosol intensive properties was much larger than day of week and diurnal variability at the four North American continental sites studied. Regional differences in annual median properties were in general much less than their seasonal variability at individual sites, requiring that studies of regional variability be conducted on a seasonal basis. That being said, there were regional differences in the relative influence of coarse mode aerosols to scattering and absorption that applied to all seasons, and hence on an annual basis as well. Median  $R_{sp}$  and  $R_{ap}$  were higher at APP than at BND and SGP for all months (Figs. 1 and 2), indicating that fine-mode particles contributed more to aerosol light scattering and absorption at APP than at SGP and BND.

Seasonal variability in  $\sigma_{sp}$  was larger than that of  $\sigma_{ap}$  at all sites except EGB (where their variability was comparable in magnitude), while the opposite was true on weekly and diurnal scales. When combined with the seasonal  $\omega_0$  vs.  $\sigma_{sp}$  relationships (Fig. 9), this indicates that the sources of  $\sigma_{sp}$  and  $\sigma_{ap}$  were most similar at EGB (primary sources) and most different at APP. The pronounced summer maxima in  $\sigma_{sp}$  observed at all sites was most noticeable at APP and EGB and was accompanied by decreases in  $b$  and increases in  $\omega_0$  at all sites, corresponding to larger, more reflective particles. Median  $\alpha_{ap}$  values much less than 1 were also observed during summer months at APP, and to a lesser degree BND. The annual cycle of biogenic VOC emissions and photochemistry likely played an important role in the seasonality of aerosol properties at APP while at EGB it was determined mainly by the frequency of episodic pollution in south/southeasterly flow from the heavily populated southern Ontario and NE US. These claims are supported by studies of aerosol chemistry at EGB (Chan et al., 2010), by aerosol chemistry and VOC measurements made at APP (Link et al., 2014) and by similar seasonality of biogenic VOCs and aerosol optical depth in the SE US (Goldstein et al., 2009). The sources of seasonality at BND and SGP appear to be a combination of photochemistry and patterns in agricultural activity, with less-pronounced  $\sigma_{sp}$  peaks

### A multi-year study of lower tropospheric aerosol variability and systematic relationships

J. P. Sherman et al.

Title Page

Abstract

Introduction

Conclusions

References

Tables

Figures

◀

▶

◀

▶

Back

Close

Full Screen / Esc

Printer-friendly Version

Interactive Discussion



during summer months possibly due to lower precursor emissions by vegetation near these sites, as compared to the forests in the SE US.

Large variability in  $\sigma_{ap}$  on weekly timescales (relative to variability in  $\sigma_{sp}$ ) was likely influenced by regional combustion sources (most likely vehicle emissions) while local and regional traffic and the diurnal cycle in boundary layer height likely contributed to the diurnal variability in  $\sigma_{ap}$ . Sunday and/or Monday minima in median  $\sigma_{ap}$  were observed for all seasons at all sites, with the exception of fall and winter at BND and spring at EGB. The days of minima  $\sigma_{ap}$  and the amplitudes of the weekly  $\sigma_{ap}$  cycles (generally on the order of  $\sim 15\text{--}30\%$ ) are similar to the weekly cycles in BC aerosol mass concentrations at IMPROVE sites in the US reported by Murphy et al. (2008), which they concluded was largely influenced by diesel emissions across the US. A lack of weekly and diurnal cycles of most aerosol intensive properties was observed for all sites, even when examined for individual seasons. Exceptions include small cycles in  $\omega_0$  (larger at EGB) that followed the  $\sigma_{ap}$  cycles. These results indicate that the amount of absorbing aerosol varied on weekly and diurnal timescales much more than the amount of scattering aerosol and that the aerosol size distributions exhibit little change on these timescales.

Large decreases in scattering (especially the  $PM_{10}$  component) at BND and SGP for the 2010–2013 period, relative to the 1996–2000 period at BND and 1997–2000 period at SGP reported by D&O2002, are in agreement with those of several other North American studies reporting decreases in aerosol light scattering, extinction, and optical depth (Collaud Coen et al., 2013; Hand et al., 2014; Li et al., 2014; Yoon, 2012). Similar (or even larger) reductions would likely have been observed at APP and EGB, based on the regional difference in aerosol loading trends reported in some of the other studies. Key indicators of aerosol size distribution have also exhibited noticeable changes at BND and SGP since D&O2002. The relative influence of coarse mode aerosols to scattering and absorption has increased at both sites, with declines in accumulation-mode aerosol more likely than increases in dust. The shift to smaller accumulation mode particles (larger  $b$ ) at both sites could be the result of less growth due to gas-

## A multi-year study of lower tropospheric aerosol variability and systematic relationships

J. P. Sherman et al.

Title Page

Abstract

Introduction

Conclusions

References

Tables

Figures

◀

▶

◀

▶

Back

Close

Full Screen / Esc

Printer-friendly Version

Interactive Discussion

to-particle conversion, given the high sensitivity of  $b$  over much of the size range of particles where this conversion is most efficient and the large reductions in gaseous precursors (most notably  $\text{SO}_2$  in the US and Canada) in the past two decades.

Sensitivity of mean aerosol intensive properties to aerosol loading was investigated on an annual basis and for individual seasons, along with selected relationships between intensive properties. In addition to their utility in constraining models and for inversions of remote sensing data, these relationships can provide information regarding aerosol sources and processes. Some observed relationships were similar for all seasons at all sites. The aerosols during low loading conditions tended to be smaller and more absorbing (higher  $b$  and lower  $\omega_0$ ) for all sites and seasons, consistent with preferential removal of large scattering particles by cloud scavenging and/or deposition. The particles tended to be larger and less absorbing for high loading conditions, consistent with particle growth. Similar relationships were reported by D&O2002 and Andrews et al. (2011). The opposing variations in  $b$  and  $\omega_0$  resulted in little change in DRFE with loading for all sites and seasons, with exception of moderate seasonal variability in  $\text{PM}_1$  DRFE at EGB. A proportional increase in  $R_{\text{sp}}$  with increasing  $\alpha_{\text{sp}}$ , along with a relatively weak relationship between  $\alpha_{\text{sp}}$  and  $\sigma_{\text{sp}}$ , provides evidence that  $\alpha_{\text{sp}}$  is a better indicator of fine-mode aerosol fraction than particle size at the four sites. The weak seasonal variability of  $R_{\text{sp}}$  and  $\alpha_{\text{sp}}$  and larger seasonal variability in  $b$  indicates that most of the seasonal changes in size distribution at the four sites were likely in the smaller accumulation-mode particles.

While systematic relationships among most variables were reasonably well-represented by the annual relationships, most involving  $\alpha_{\text{ap}}$  varied highly with season, both in magnitude and shape of the curves. Mean  $\alpha_{\text{ap}}$  was much lower during summer months and values below 1 were associated with nearly all loading levels at APP and with higher loading levels at BND. Similar behavior was observed at SGP during fall. Values of  $\alpha_{\text{ap}} < 1$  were associated with high  $\omega_0$  and higher relative influence from fine-mode aerosols. High  $\omega_0$  is associated with smaller  $b$  (Fig. 10), leading us to hypothesize condensation of organic and inorganic matter onto BC aerosols as the

## A multi-year study of lower tropospheric aerosol variability and systematic relationships

J. P. Sherman et al.

Title Page

Abstract

Introduction

Conclusions

References

Tables

Figures

◀

▶

◀

▶

Back

Close

Full Screen / Esc

Printer-friendly Version

Interactive Discussion



## A multi-year study of lower tropospheric aerosol variability and systematic relationships

J. P. Sherman et al.

Title Page

Abstract

Introduction

Conclusions

References

Tables

Figures

◀

▶

◀

▶

Back

Close

Full Screen / Esc

Printer-friendly Version

Interactive Discussion

- Andrews, E., Sheridan, P. J., Fiebig, M., McComiskey, A., Ogren, J. A., Arnott, P., Covert, D., Elleman, R., Gasparini, R., Collins, D., Jonsson, H., Schmid, B., and Wang, J.: Comparison of methods for deriving aerosol asymmetry parameter, *J. Geophys. Res.*, 111, D05S04, doi:10.1029/2004JD005734, 2006.
- 5 Andrews, E., Ogren, J. A., Bonasoni, P., Marinoni, A., Cuevas, E., Rodriguez, S., Sun, J. Y., Jaffe, D. A., Fischer, E. V., Baltensperger, U., Weingartner, E., Collaud Coen, M., Sharma, S., Macdonald, A. M., Leaitch, W. R., Lin, N.-H., Laj, P., Arsov, T., Kalapov, I., Jefferson, A., and Sheridan, P.: Climatology of aerosol radiative properties in the free troposphere, *Atmos. Res.*, 102, 365–393, 2011.
- 10 Bergstrom, R. W., Pilewskie, P., Russell, P. B., Redemann, J., Bond, T. C., Quinn, P. K., and Sierau, B.: Spectral absorption properties of atmospheric aerosols, *Atmos. Chem. Phys.*, 7, 5937–5943, doi:10.5194/acp-7-5937-2007, 2007.
- Bond, T. C., Anderson, T. L., and Campbell, D.: Calibration and inter-comparison of filter-based measurements of visible light absorption by aerosols, *Aerosol Sci. Tech.*, 30, 582–600, doi:10.1080/027868299304435, 1999.
- 15 Cazorla, A., Bahadur, R., Suski, K. J., Cahill, J. F., Chand, D., Schmid, B., Ramanathan, V., and Prather, K. A.: Relating aerosol absorption due to soot, organic carbon, and dust to emission sources determined from in-situ chemical measurements, *Atmos. Chem. Phys.*, 13, 9337–9350, doi:10.5194/acp-13-9337-2013, 2013.
- 20 Chan, T. W., Huang, L., Leaitch, W. R., Sharma, S., Brook, J. R., Slowik, J. G., Abbatt, J. P. D., Brickell, P. C., Liggio, J., Li, S.-M., and Moosmüller, H.: Observations of OM/OC and specific attenuation coefficients (SAC) in ambient fine PM at a rural site in central Ontario, Canada, *Atmos. Chem. Phys.*, 10, 2393–2411, doi:10.5194/acp-10-2393-2010, 2010.
- Clarke, A., McNaughton, C., Kapustin, V., Shinozuka, V., Howell, S., Dibb, J., Zhou, J., Anderson, B., Brekhovskikh, V., Turner, H., and Pinkerton, M.: Biomass burning and pollution aerosol over North America: organic components and their influence on spectral optical properties and humidification response, *J. Geophys. Res.*, 112, D12S18, doi:10.1029/2006JD007777, 2007.
- 25 Collaud Coen, M., Weingartner, E., Nyeki, S., Cozic, J., Henning, S., Verheggen, B., Gehrig, R., and Baltensperger, U.: Long-term trend analysis of aerosol variables at the high-alpine site Jungfraujoch, *J. Geophys. Res.*, 112, D13213, doi:10.1029/2006JD007995, 2007.
- Collaud Coen, M., Andrews, E., Asmi, A., Baltensperger, U., Bukowiecki, N., Day, D., Fiebig, M., Fjaeraa, A. M., Flentje, H., Hyvärinen, A., Jefferson, A., Jennings, S. G., Kouvarakis, G.,

## A multi-year study of lower tropospheric aerosol variability and systematic relationships

J. P. Sherman et al.

Title Page

Abstract

Introduction

Conclusions

References

Tables

Figures

◀

▶

◀

▶

Back

Close

Full Screen / Esc

Printer-friendly Version

Interactive Discussion

Lihavainen, H., Lund Myhre, C., Malm, W. C., Mihapopoulos, N., Molenaar, J. V., O'Dowd, C., Ogren, J. A., Schichtel, B. A., Sheridan, P., Virkkula, A., Weingartner, E., Weller, R., and Laj, P.: Aerosol decadal trends – Part 1: In-situ optical measurements at GAW and IMPROVE stations, *Atmos. Chem. Phys.*, 13, 869–894, doi:10.5194/acp-13-869-2013, 2013.

5 Costabile, F., Barnaba, F., Angelini, F., and Gobbi, G. P.: Identification of key aerosol populations through their size and composition resolved spectral scattering and absorption, *Atmos. Chem. Phys.*, 13, 2455–2470, doi:10.5194/acp-13-2455-2013, 2013.

Delene, D. J. and Ogren, J. A.: Variability of aerosol optical properties at four North American surface monitoring sites, *J. Atmos. Sci.*, 59, 1135–1150, 2002.

10 Dubovik, O., Smirnov, A., Holben, B. N., King, M. D., Kaufman, Y. J., Eck, T. F., and Slutsker, I.: Accuracy assessments of aerosol optical properties retrieved from Aerosol Robotic Network (AERONET) Sun and sky radiance measurements, *J. Geophys. Res.*, 105, 9791–9806, 2000.

Fast, J., Zhang, Q., Tilp, A., Shippert, T., Parworth, C., and Mei, F.: Organic aerosol component (OACOMP): an ARM value-added product, ARM Climate Science Research Facility report, DOE/SC-ARM-TR-131, available at: [https://www.arm.gov/publications/tech\\_reports/doe-sc-arm-tr-131.pdf](https://www.arm.gov/publications/tech_reports/doe-sc-arm-tr-131.pdf) (last access: 25 October 2014), 2013.

15 Goldstein, A. H., Koven, C. D., Heald, C. L., and Fung, I. Y.: Biogenic carbon and anthropogenic pollutants combine to form a cooling haze over the southeastern United States, *P. Natl. Acad. Sci. USA*, 106, 8835–8840, doi:10.1073/pnas.0904128106, 2009.

20 Gyawali, M., Arnott, W. P., Lewis, K., and Moosmüller, H.: In situ aerosol optics in Reno, NV, USA during and after the summer 2008 California wildfires and the influence of absorbing and non-absorbing organic coatings on spectral light absorption, *Atmos. Chem. Phys.*, 9, 8007–8015, doi:10.5194/acp-9-8007-2009, 2009.

25 Hand, J. L., Copeland, S. A., McDade, C. E., Day, D. E., Moore Jr., C. T., Dillner, A. M., Pitchford, M. L., Indresand, H., Schichtel, B. A., Malm, W. C., and Watson, J. G.: Spatial and seasonal patterns and temporal variability of haze and its constituents in the United States: Report V, CIRA Report, ISSN: 0737-5352-87, Fort Collins, CO, USA, 2011.

30 Hand, J. L., Schichtel, B. A., Malm, W. C., and Pitchford, M. L.: Particulate sulfate ion concentration and SO<sub>2</sub> emission trends in the United States from the early 1990s through 2010, *Atmos. Chem. Phys.*, 12, 10353–10365, doi:10.5194/acp-12-10353-2012, 2012.

## A multi-year study of lower tropospheric aerosol variability and systematic relationships

J. P. Sherman et al.

Title Page

Abstract

Introduction

Conclusions

References

Tables

Figures

◀

▶

◀

▶

Back

Close

Full Screen / Esc

Printer-friendly Version

Interactive Discussion

- Hand, J. L., Schichtel, B. A., Malm, W. C., Copeland, S., Molenaar, J. V., Frank, N., and Pitchford, M.: Widespread reductions in haze across the United States from the early 1990s through 2011, *Atmos. Environ.*, 94, 671–679, doi:10.1016/j.atmosenv.2014.05.062, 2014.
- Hansen, J., Sato, M., and Ruedy, R.: Radiative forcing and climate response, *J. Geophys. Res.*, 102, 6831–6864, 1997.
- Haywood, J. M. and Shine, K. P.: The effect of anthropogenic sulfate and soot aerosol on the clear sky planetary radiation budget, *Geophys. Res. Lett.*, 22, 603–606, doi:10.1029/95GL00075, 1995.
- Holben, B. N., Eck, T. F., Slutsker, I., Tanre, D., Buis, J. P., Setzer, A., Vermote, E., Reagan, J. A., Kaufman, Y. J., Nakajima, T., Lavenu, F., Janowiak, I., and Smirnov, A.: AERONET – a federated instrument network and data archive for aerosol characterization, *Remote Sens. Environ.*, 66, 1–16, 1998.
- Kahn, R. A., Yu, H., Schwartz, S. E., Chin, M., Feingold, G., Remer, L. A., Rind, D., Halthore, R., and DeCola, P.: Introduction, in: *Atmospheric Aerosol Properties and Climate Impacts*, A Report by the US Climate Change Science Program and the Subcommittee on Global Change Research, edited by: Chin, M., Kahn, R. A., and Schwartz, S. E., National Aeronautics and Space Administration, Washington DC, USA, 9–20, 2009.
- Kleinman, L. I., Daum, P. H., Lee, Y., Senum, G. I., Springston, S. R., Wang, J., Berkowitz, C., Hubbe, J., Zaveri, R. A., Brechtel, F. J., Jayne, J., Onasch, T. B., and Worsnop, D.: Aircraft observations of aerosol composition and ageing in New England and Mid-Atlantic States during the summer 2002 New England Air Quality Study field campaign, *J. Geophys. Res.*, 112, D09310, doi:10.1029/2006JD007786, 2007.
- Kohler, C. H., Trautmann, T., Lindermeir, E., Vreeling, W., Lieke, K., Kandler, K., Weinzierl, B., Groß, S., Tesche, M., and Wendisch, M.: Thermal IR radiative properties of mixed mineral dust and biomass aerosol during SAMUM-2, *Tellus B*, 63, 751–769, doi:10.1111/j.1600-0889.2011.00563.x, 2011.
- Koloutsou-Vakakis, S., Carrico, C. M., Kus, P., Rood, M. J., Li, Z., Shrestha, R., Ogren, J. A., Chow, J. C., and Watson, J. G.: Aerosol properties at a midlatitude Northern Hemisphere continental site, *J. Geophys. Res.*, 106, 3019–3032, doi:10.1029/2000JD900126, 2001.
- Lack, D. A., Cappa, C. D., Covert, D. S., Baynard, T., Massoli, P., Sierau, B., Bates, T. S., Quinn, P. K., Lovejoy, E. R., and Ravishankara, A. R.: Bias in filter-based aerosol light absorption measurements due to organic aerosol loading: evidence from ambient measurements, *Aerosol Sci. Tech.*, 42, 1033–1041, doi:10.1080/02786820802389277, 2008.

**A multi-year study of  
lower tropospheric  
aerosol variability  
and systematic  
relationships**

J. P. Sherman et al.

Title Page

Abstract

Introduction

Conclusions

References

Tables

Figures

◀

▶

◀

▶

Back

Close

Full Screen / Esc

Printer-friendly Version

Interactive Discussion



Lack, D. A., Cappa, C. D., Cross, E. S., Massoli, P., Ahern, A. T., Davidovits, P., and Onasch, T. B.: Absorption enhancement of coated absorbing aerosols: validation of the photo-acoustic technique for measuring the enhancement, *Aerosol Sci. Tech.*, 43, 1006–1012, doi:10.1080/02786820903117932, 2009.

5 Levy, R. C., Remer, L. A., Kleidman, R. G., Mattoo, S., Ichoku, C., Kahn, R., and Eck, T. F.: Global evaluation of the Collection 5 MODIS dark-target aerosol products over land, *Atmos. Chem. Phys.*, 10, 10399–10420, doi:10.5194/acp-10-10399-2010, 2010.

Li, J., Carlson, B. E., Dubovik, O., and Laciš, A. A.: Recent trends in aerosol optical properties derived from AERONET measurements, *Atmos. Chem. Phys. Discuss.*, 14, 14351–14397, doi:10.5194/acpd-14-14351-2014, 2014.

10 Link, M. F., Zhou, Y., Taubman, B. F., Sherman, J. P., Sive, B. C., Morrow, H., Krintz, I., Robertson, L., Cook, R., Stocks, J., and West, M.: Estimating background secondary organic aerosol in the southeastern United States from a regionally representative site, *J. Atmos. Chem.*, submitted, 2014.

15 Malm, W. C., Schichtel, B. A., Pitchford, M. L., Ashbaugh, L. L., and Eldred, R. A.: Spatial and monthly trends in speciated fine particle concentration in the United States, *J. Geophys. Res.*, 109, D03306, doi:10.1029/2003JD003739, 2004.

Massoli, P., Murphy, D. M., Lack, D. A., Baynard, T., Brock, C. A., and Lovejoy, E. R.: Uncertainty in light scattering measurements by TSI nephelometer: results from laboratory studies and implications for ambient measurements, *Aerosol Sci. Tech.*, 43, 1064–1074, doi:10.1080/02786820903156542, 2009.

20 Murphy, D. M., Capps, S. L., Daniel, J. S., Frost, G. J., and White, W. H.: Weekly patterns of aerosol in the United States, *Atmos. Chem. Phys.*, 8, 2729–2739, doi:10.5194/acp-8-2729-2008, 2008.

25 Murphy, D. M., Chow, J. C., Leibensperger, E. M., Malm, W. C., Pitchford, M., Schichtel, B. A., Watson, J. G., and White, W. H.: Decreases in elemental carbon and fine particle mass in the United States, *Atmos. Chem. Phys.*, 11, 4679–4686, doi:10.5194/acp-11-4679-2011, 2011.

Ogren, J. A.: Comment on “Calibration and Intercomparison of Filter-Based Measurements of Visible Light Absorption by Aerosols”, *Aerosol Sci. Tech.*, 44, 589–591, doi:10.1080/02786826.2010.482111, 2010.

30 Ogren, J. A., Wendell, J., Sheridan, P. J., Hageman, D., and Jefferson, A.: Continuous light absorption photometer performance, ASR Science Team Meeting, Potomac, Md, USA, 18–21

## A multi-year study of lower tropospheric aerosol variability and systematic relationships

J. P. Sherman et al.

Title Page

Abstract

Introduction

Conclusions

References

Tables

Figures

◀

▶

◀

▶

Back

Close

Full Screen / Esc

Printer-friendly Version

Interactive Discussion

March, available at: <http://asr.science.energy.gov/meetings/stm/posters/view?id=781> (last access: 26 October 2014), 2013.

Quinn, P. K., Bates, T. S., Baynard, T., Clarke, A. D., Onasch, T. B., Wang, W., Rood, M., Andrews, E., Allan, J., Carrico, C. M., Coffman, D., and Worsnop, D.: Impact of particulate organic matter on the relative humidity dependence of light scattering: a simplified parameterization, *Geophys. Res. Lett.*, 32, L22809, doi:10.1029/2005GL024322, 2005.

Remer, L. A. and Kaufman, Y. J.: Dynamic aerosol model: urban/industrial aerosol, *J. Geophys. Res.*, 103, 13859–13871, 1998.

Schuster, G. L., Dubovik, O., and Holben, B. N.: Angstrom exponent and bimodal aerosol size distributions, *J. Geophys. Res.*, 111, D07207, doi:10.1029/2005JD006328, 2006.

Seinfeld, J. H. and Pandis, S. N.: *Atmospheric Chemistry and Physics: From Air Pollution to Climate Change*, 2nd edn., John Wiley & Sons, New York, New York, USA, 1998.

Sheridan, P. J. and Ogren, J. A.: Observations of the vertical and regional variability of aerosol optical properties over central and eastern North America, *J. Geophys. Res.*, 104, 16793–16805, doi:10.1029/1999JD900241, 1999.

Sheridan, P. J., Delene, D. J., and Ogren, J. A.: Four years of continuous surface aerosol measurements from the Department of Energy's Atmospheric Radiation Measurement Program Southern Great Plains Cloud and Radiation Testbed site, *J. Geophys. Res.*, 106, 20735–20747, doi:10.1029/2001JD000785, 2001.

Sheridan, P. J., Jefferson, A., and Ogren, J. A.: Spatial variability of submicrometer aerosol radiative properties over the Indian Ocean during INDOEX, *J. Geophys. Res.*, 107, 8011, doi:10.1029/2000JD000166, 2002.

Sheridan, P. J., Andrews, E., Ogren, J. A., Tackett, J. L., and Winker, D. M.: Vertical profiles of aerosol optical properties over central Illinois and comparison with surface and satellite measurements, *Atmos. Chem. Phys.*, 12, 11695–11721, doi:10.5194/acp-12-11695-2012, 2012.

U.S. Environmental Protection Agency: Health Assessment Document for Diesel Engine Exhaust, National Center for Environmental Assessment, Washington DC, EPA/600/8-90/057F, available at: <http://www.epa.gov/ncea> (access date: 26 October 2014), 2002.

van de Hulst, H. C.: *Light Scattering by Small Particles*, John Wiley and Sons, New York, 1957.

Wiscombe, W. J. and Grams, G. W.: The backscattered fraction in two-stream approximations, *J. Atmos. Sci.*, 33, 2440–2451, 1976.

**A multi-year study of lower tropospheric aerosol variability and systematic relationships**

J. P. Sherman et al.

Title Page

Abstract

Introduction

Conclusions

References

Tables

Figures

◀

▶

◀

▶

Back

Close

Full Screen / Esc

Printer-friendly Version

Interactive Discussion



- Yoon, J., von Hoyningen-Huene, W., Kokhanovsky, A. A., Vountas, M., and Burrows, J. P.: Trend analysis of aerosol optical thickness and Ångström exponent derived from the global AERONET spectral observations, *Atmos. Meas. Tech.*, 5, 1271–1299, doi:10.5194/amt-5-1271-2012, 2012.
- 5 Yu, H., Kaufman, Y. J., Chin, M., Feingold, G., Remer, L. A., Anderson, T. L., Balkanski, Y., Bellouin, N., Boucher, O., Christopher, S., DeCola, P., Kahn, R., Koch, D., Loeb, N., Reddy, M. S., Schulz, M., Takemura, T., and Zhou, M.: A review of measurement-based assessments of the aerosol direct radiative effect and forcing, *Atmos. Chem. Phys.*, 6, 613–666, doi:10.5194/acp-6-613-2006, 2006.
- 10 Yu, H., Quinn, P. K., Feingold, G., Remer, L. A., Kahn, R. A., Chin, M., and Schwartz, S. E.: Remote sensing and in situ measurements of aerosol properties, burdens, and radiative forcing, in: *Atmospheric Aerosol Properties and Climate Impacts*, a Report by the US Climate Change Science Program and the Subcommittee on Global Change Research, edited by: Chin, M., Kahn, R. A., and Schwartz, S. E., National Aeronautics and Space Administration, Washington DC, USA, 21–54, 2009.
- 15 Zhang, X., Hecobian, A., Zheng, M., Frank, N. H., and Weber, R. J.: Biomass burning impact on  $PM_{2.5}$  over the southeastern US during 2007: integrating chemically speciated FRM filter measurements, MODIS fire counts and PMF analysis, *Atmos. Chem. Phys.*, 10, 6839–6853, doi:10.5194/acp-10-6839-2010, 2010.

## A multi-year study of lower tropospheric aerosol variability and systematic relationships

J. P. Sherman et al.

**Table 1.** Parameters and equations used to calculate aerosol optical properties. Constants and parameters used in the formula to calculate globally-averaged top-of-atmosphere direct radiative forcing (DRFE) are also included and are denoted with \*.

Parameter	Equation (or value)
Extinction coefficient	$\sigma_{\text{ep}} = \sigma_{\text{sp}} + \sigma_{\text{ap}}$
Single-scattering albedo	$\omega_0 = \sigma_{\text{sp}} / \sigma_{\text{ep}} = \sigma_{\text{sp}} / (\sigma_{\text{sp}} + \sigma_{\text{ap}})$
Hemispheric backscatter fraction	$b = \sigma_{\text{bsp}} / \sigma_{\text{sp}}$
Scattering Ångström exponent	$\alpha_{\text{sp}} = -\log(\sigma_{\text{sp}}(\lambda_1) / \sigma_{\text{sp}}(\lambda_2)) / \log(\lambda_1 / \lambda_2)$
Absorption Ångström exponent	$\alpha_{\text{ap}} = -\log(\sigma_{\text{ap}}(\lambda_1) / \sigma_{\text{ap}}(\lambda_2)) / \log(\lambda_1 / \lambda_2)$
Sub-micron scattering fraction	$R_{\text{sp}} = \sigma_{\text{sp,PM}_1} / \sigma_{\text{sp,PM}_{10}}$
Sub-micron absorption fraction	$R_{\text{ap}} = \sigma_{\text{ap,PM}_1} / \sigma_{\text{ap,PM}_{10}}$
Direct Radiative Forcing Efficiency	$\text{DRFE} = \text{DRF} / \tau = -\text{DS}_0 T_{\text{atm}}^2 (1 - A_c) \beta \omega_0 \times \left[ (1 - R_s)^2 - (2R_s / \omega_0 \beta) (1 - \omega_0) \right]$
Upscatter Fraction*	$\beta = 0.0817 + 1.8495 \times b - 2.9682 \times b^2$
Fractional Day Length*	$D = 0.50$ (globally-averaged)
Solar Constant*	$S_0 = 1370 \text{ W m}^{-2}$
Atmospheric Transmission*	$T_{\text{atm}} = 0.76$ (globally-averaged)
Cloud Fraction*	$A_c = 0.60$ (globally-averaged)
Spectrally-averaged surface albedo**	$R_s = 0.15$ (globally-averaged)

Title Page

Abstract

Introduction

Conclusions

References

Tables

Figures

◀

▶

◀

▶

Back

Close

Full Screen / Esc

Printer-friendly Version

Interactive Discussion



## A multi-year study of lower tropospheric aerosol variability and systematic relationships

J. P. Sherman et al.

**Table 2.** Sites, instruments and data period included in the study, listed from west to east. Aerosol sampling size cuts and the instrument used to measure absorption is also included. All sites used a TSI 3563 3- $\lambda$  nephelometer<sup>1</sup> to measure total scattering and hemispheric backscattering.

Site	Lat/Long (°)	Elev. (m a.s.l.)	Yrs. Data used	#Hrs used 2010–2013	Size Cut ( $\mu\text{m}$ )	Absorption Instrument (Dates used)
SGP	36.6° N, 97.5° W	315	1997–2013	32 971 ( $\sigma_{\text{sp}}$ ), 25 140 ( $\sigma_{\text{ap}}$ )	1.10	1- $\lambda$ PSAP <sup>2</sup> (Apr 1997–Mar 2005), 3- $\lambda$ PSAP <sup>3</sup> (Apr 2005–Dec 2013)
BND	40.0° N, 88.4° W	230	1996–2013	33 449 ( $\sigma_{\text{sp}}$ ), 32 040 ( $\sigma_{\text{ap}}$ )	1.10	1- $\lambda$ PSAP (Sep 1996–Feb 2006), 3- $\lambda$ PSAP (Mar 2006–Feb 2012), 3- $\lambda$ CLAP <sup>4</sup> (Mar 2012–Dec 2013)
EGB	44.2° N, 79.8° W	253	2010–2013	32 448 ( $\sigma_{\text{sp}}$ ), 26 304 ( $\sigma_{\text{ap}}$ )	1	1- $\lambda$ PSAP
APP	36.2° N, 81.7° W	1080	2010–2013	34 220 ( $\sigma_{\text{sp}}$ ), 34 178 ( $\sigma_{\text{ap}}$ )	1.10	3- $\lambda$ PSAP

<sup>1</sup> 3- $\lambda$  TSI nephelometer measures at  $\lambda = 450, 550, 700$  nm.

<sup>2</sup> 1- $\lambda$  PSAP measures at 565 nm, adjusted to 550 nm using Bond et al. (1999) correction.

<sup>3</sup> 3- $\lambda$  PSAP measures at 467, 530, 660 nm.

<sup>4</sup> 3- $\lambda$  CLAP measures at 467, 529, 653 nm.

Title Page

Abstract

Introduction

Conclusions

References

Tables

Figures



Back

Close

Full Screen / Esc

Printer-friendly Version

Interactive Discussion



**A multi-year study of lower tropospheric aerosol variability and systematic relationships**

J. P. Sherman et al.

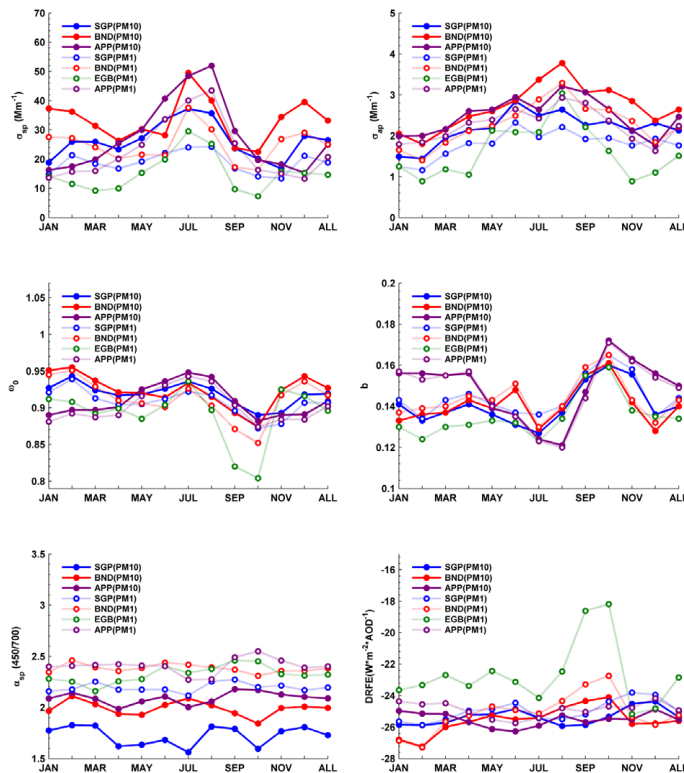


**Figure 1.** Annual cycle of median PM<sub>10</sub> and PM<sub>1</sub> aerosol light scattering coefficient ( $\sigma_{sp}$ ), absorption coefficient ( $\sigma_{ap}$ ), single-scattering albedo ( $\omega_0$ ), hemispheric backscatter fraction ( $b$ ), scattering Ångström exponent ( $\alpha_{sp}$ ) and direct radiative forcing efficiency (DRFE) at SGP, BND, APP, and EGB (PM<sub>1</sub> only) for years 2010–2013. The values corresponding to “ALL” are median values for the entire 2010–2013 period (all months). All displayed quantities are for wavelength of 550 nm except for  $\alpha_{sp}$ , which is calculated using the 450 and 700 nm wavelengths.

Title Page

Abstract Introduction

Conclusions References

Tables Figures

◀ ▶

◀ ▶

Back Close

Full Screen / Esc

Printer-friendly Version

Interactive Discussion



## A multi-year study of lower tropospheric aerosol variability and systematic relationships

J. P. Sherman et al.

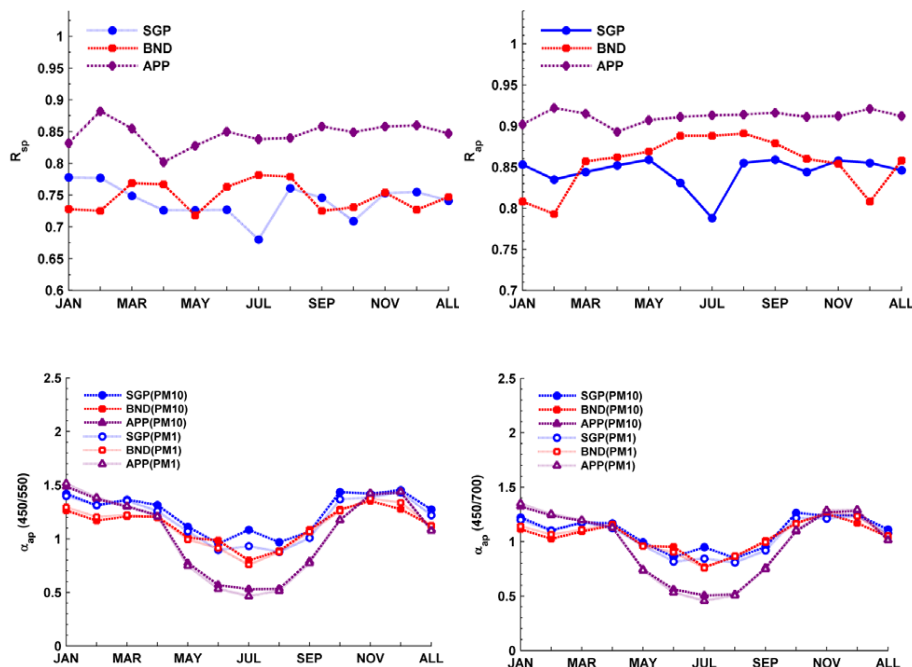


**Figure 2.** Annual cycle of median sub-1 μm aerosol scattering and absorption fractions ( $R_{sp}$  and  $R_{ap}$ ) at 550 nm, along with median PM<sub>10</sub> and PM<sub>1</sub> aerosol absorption Ångström exponents ( $\alpha_{ap}$ ), using the 450/550 nm and 450/700 nm pairs, for years 2010–2013. The values corresponding to “ALL” are median values for the entire 2010–2013 period (all months).

Title Page

Abstract

Introduction

Conclusions

References

Tables

Figures

◀

▶

◀

▶

Back

Close

Full Screen / Esc

Printer-friendly Version

Interactive Discussion

## A multi-year study of lower tropospheric aerosol variability and systematic relationships

J. P. Sherman et al.

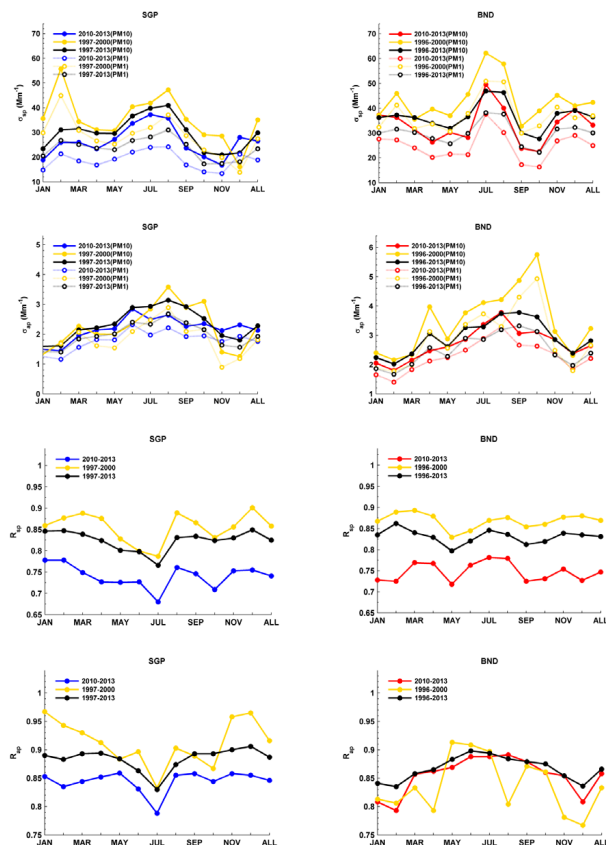


**Figure 3.** Annual cycle of median  $\text{PM}_{10}$  and  $\text{PM}_1$  aerosol light scattering coefficient ( $\sigma_{\text{sp}}$ ), absorption coefficient ( $\sigma_{\text{ap}}$ ), and sub-micrometer scattering and absorption fractions ( $R_{\text{sp}}$  and  $R_{\text{ap}}$ , respectively) at 550 nm at SGP and BND for different periods. Data points corresponding to “ALL” are median values over the entire period.

## A multi-year study of lower tropospheric aerosol variability and systematic relationships

J. P. Sherman et al.

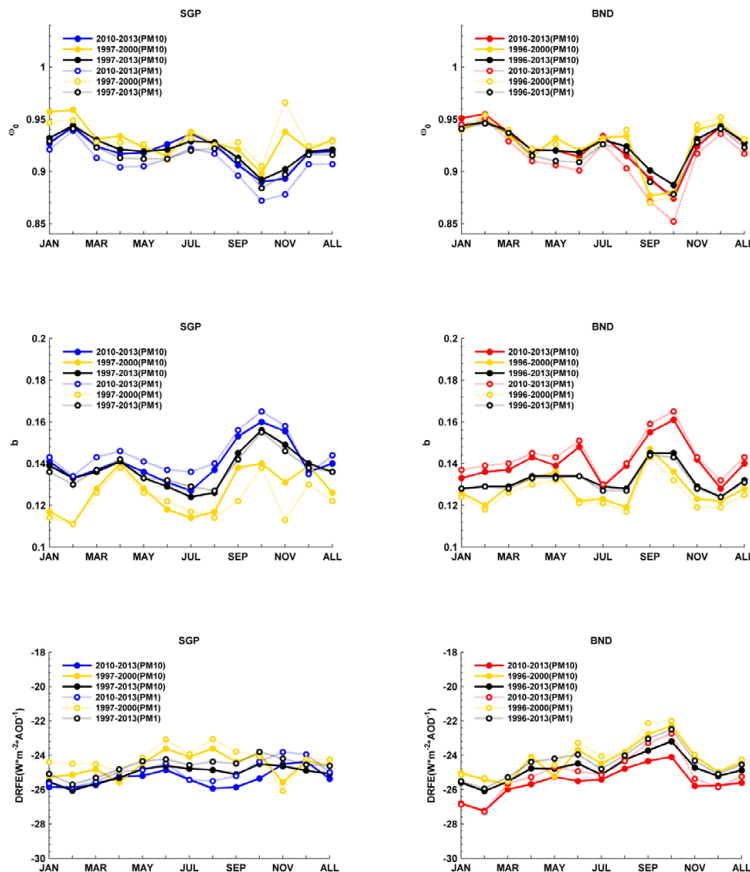


**Figure 4.** Annual cycle of median  $PM_{10}$  and  $PM_1$  aerosol single-scattering albedo ( $\omega_0$ ), hemispheric backscatter coefficient ( $b$ ), and direct radiative forcing efficiency (DRFE) at 550 nm at SGP and BND for different periods. The values corresponding to “ALL” are median values over the entire period.

[Title Page](#)
[Abstract](#)
[Introduction](#)
[Conclusions](#)
[References](#)
[Tables](#)
[Figures](#)
[Back](#)
[Close](#)
[Full Screen / Esc](#)
[Printer-friendly Version](#)
[Interactive Discussion](#)

**A multi-year study of lower tropospheric aerosol variability and systematic relationships**

J. P. Sherman et al.

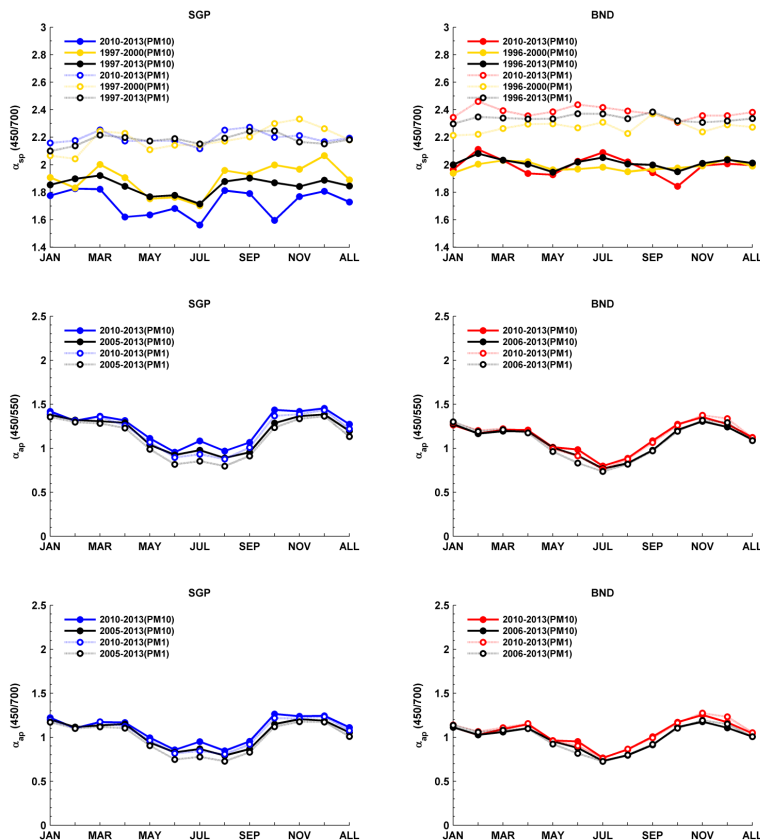


**Figure 5.** Annual cycle of median  $PM_{10}$  and  $PM_1$  aerosol scattering and absorption Ångström exponent ( $\alpha_{sp}$ , and  $\alpha_{ap}$ ), at SGP and BND for different periods, calculated using the wavelengths (in nm) denoted on y axis. The values corresponding to “ALL” are median values over the entire period. The 3- $\lambda$  absorption measurements were initiated in 2005 at SGP and 2006 at BND so no comparisons with D&O2002 are available for  $\alpha_{ap}$ .

Title Page

Abstract

Introduction

Conclusions

References

Tables

Figures

◀

▶

◀

▶

Back

Close

Full Screen / Esc

Printer-friendly Version

Interactive Discussion



## A multi-year study of lower tropospheric aerosol variability and systematic relationships

J. P. Sherman et al.

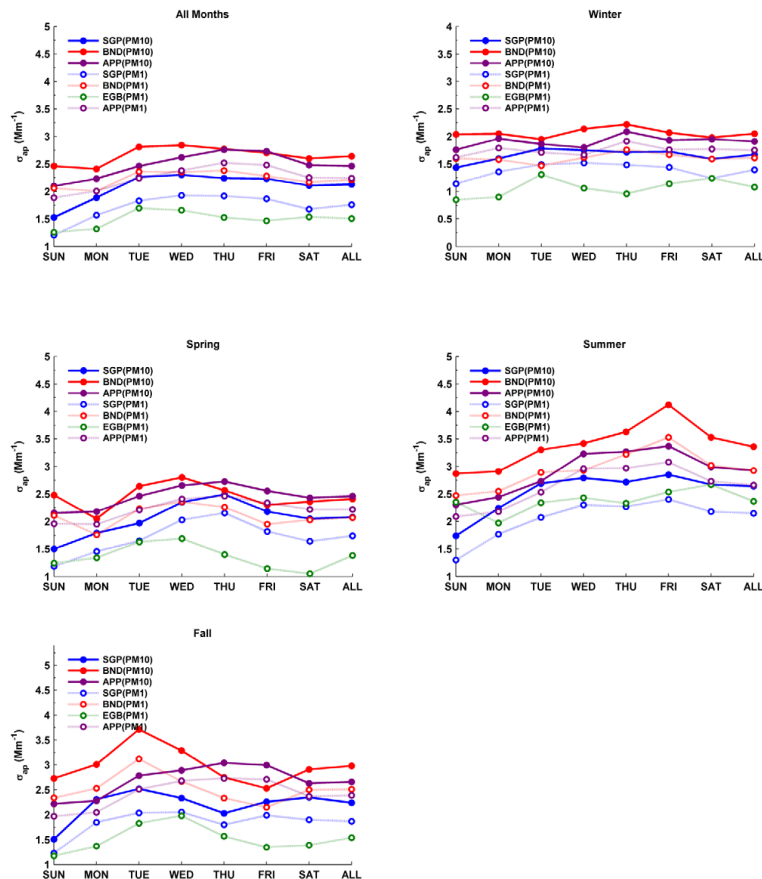


**Figure 6.** Weekly cycle of median  $\text{PM}_{10}$  and  $\text{PM}_1$  aerosol absorption coefficient ( $\sigma_{\text{ap}}$ ) at 550 nm for full years (all months) and broken down by season, over the period 2010–2013. Months comprising the seasons are DJF (winter), MAM (spring), JJA (summer), and SON (fall). The values corresponding to “ALL” are median values over the entire period for that particular season.

Title Page

Abstract

Introduction

Conclusions

References

Tables

Figures

◀

▶

◀

▶

Back

Close

Full Screen / Esc

Printer-friendly Version

Interactive Discussion

## A multi-year study of lower tropospheric aerosol variability and systematic relationships

J. P. Sherman et al.

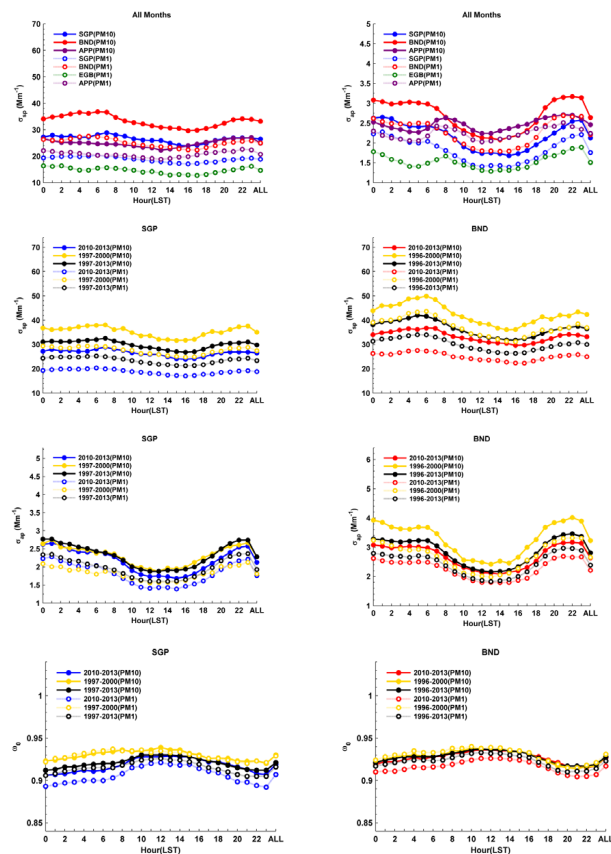


**Figure 7.** Diurnal cycle of median PM<sub>10</sub> and PM<sub>1</sub> aerosol light scattering coefficient ( $\sigma_{sp}$ ) and absorption coefficient ( $\sigma_{ap}$ ) at 550 nm for all months of the 2010–2013 period at all sites, along with median  $\sigma_{sp}$ ,  $\sigma_{ap}$ , and single-scattering albedo ( $\omega_0$ ) at 550 nm for different periods at SGP and BND. The values corresponding to “ALL” are median values over the entire period.

## A multi-year study of lower tropospheric aerosol variability and systematic relationships

J. P. Sherman et al.

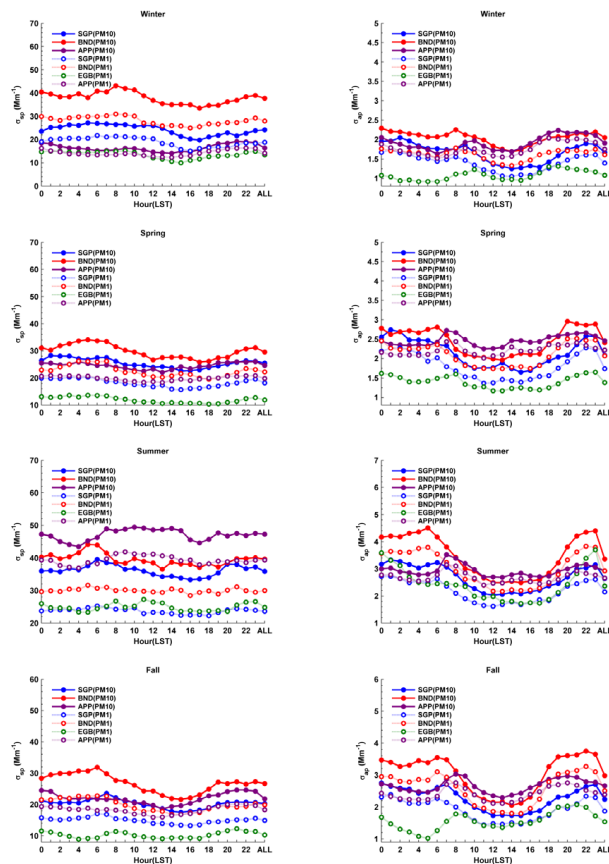


**Figure 8.** Diurnal cycle of median  $\text{PM}_{10}$  and  $\text{PM}_1$  aerosol scattering coefficient ( $\sigma_{\text{sp}}$ ) and absorption coefficient ( $\sigma_{\text{ap}}$ ) at 550 nm for all sites, broken down by individual seasons, during the period 2010–2013. Months comprising the seasons are DJF (winter), MAM (spring), JJA (summer), and SON (fall). The values corresponding to “ALL” are median values over the given seasons for the entire period.

Title Page	
Abstract	Introduction
Conclusions	References
Tables	Figures
◀	▶
◀	▶
Back	Close
Full Screen / Esc	
Printer-friendly Version	
Interactive Discussion	

## A multi-year study of lower tropospheric aerosol variability and systematic relationships

J. P. Sherman et al.

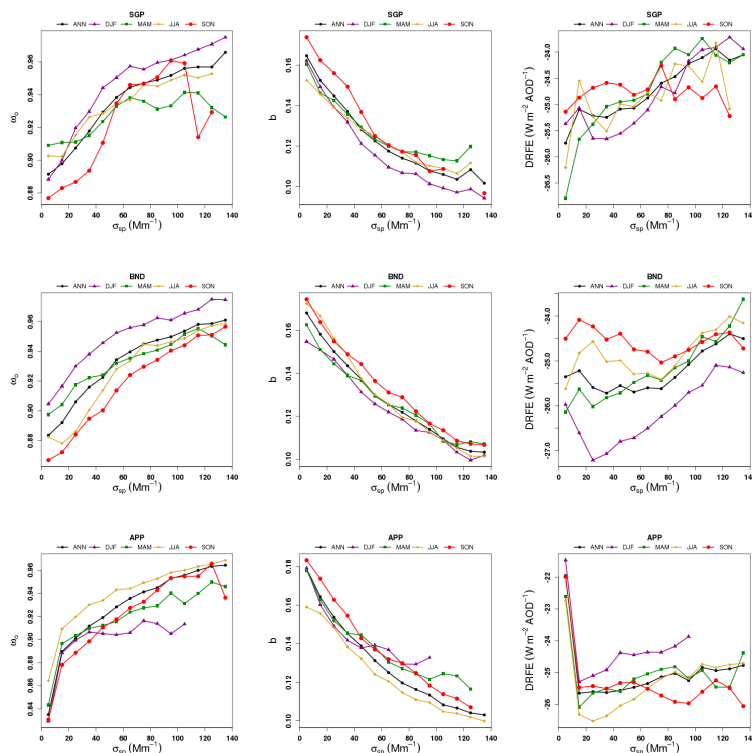


**Figure 9.** Mean single-scattering albedo ( $\omega_0$ ), hemispheric backscatter fraction ( $b$ ), and direct radiative forcing efficiency (DRFE) vs. aerosol light scattering coefficient ( $\sigma_{sp}$ ) for individual seasons and full annual cycles at SGP, BND, EGB, and APP over the years 2010–2013. Months comprising the seasons are DJF (winter), MAM (spring), JJA (summer), and SON (fall). The “ANN” curve in each plot represents the curve for all seasons. The mean values were calculated over  $10 \text{ M m}^{-1} \sigma_{sp}$  bins. All displayed quantities are for wavelength of 550 nm. Displayed curves are for  $\text{PM}_{10}$  at SGP, BND, and APP and for  $\text{PM}_1$  at EGB.

Title Page

Abstract

Introduction

Conclusions

References

Tables

Figures



Back

Close

Full Screen / Esc

Printer-friendly Version

Interactive Discussion

**A multi-year study of lower tropospheric aerosol variability and systematic relationships**

J. P. Sherman et al.

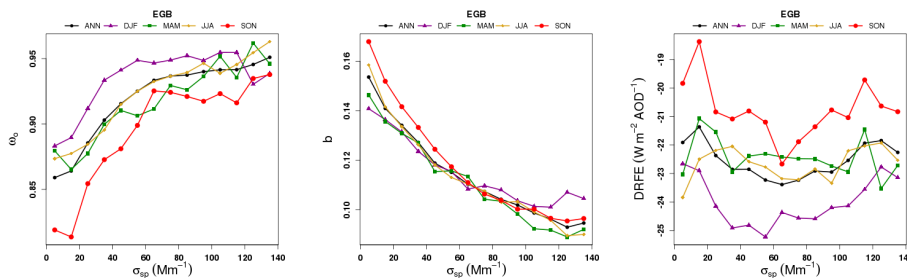


Figure 9. Continued.

Title Page	
Abstract	Introduction
Conclusions	References
Tables	Figures
◀	▶
◀	▶
Back	Close
Full Screen / Esc	
Printer-friendly Version	
Interactive Discussion	



## A multi-year study of lower tropospheric aerosol variability and systematic relationships

J. P. Sherman et al.

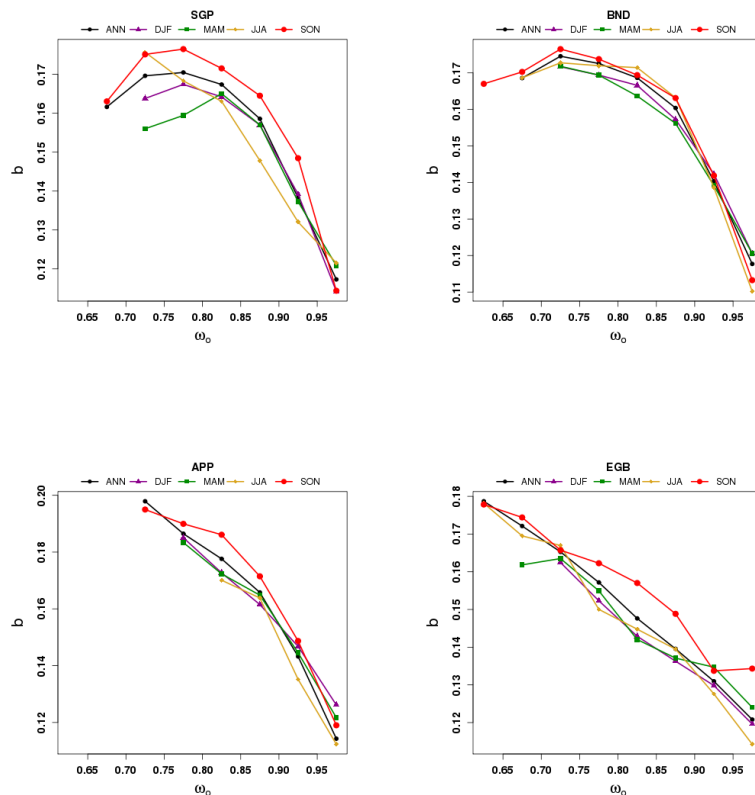


**Figure 10.** Mean hemispheric backscatter fraction ( $b$ ) vs. single scattering albedo ( $\omega_0$ ) for individual seasons and full annual cycles at SGP, BND, APP, and EGB over the years 2010–2013. Months comprising the seasons are DJF (winter), MAM (spring), JJA (summer), and SON (fall). The “ANN” curve in each plot represents the curve for all seasons. Displayed curves are for  $\text{PM}_{10}$  at SGP, BND, and APP and for  $\text{PM}_1$  at EGB. The mean values were calculated over  $10 \text{ M m}^{-1} \sigma_{\text{sp}}$  bins and over  $0.05 \omega_0$  bins. All displayed quantities are for wavelength of  $550 \text{ nm}$ .

## A multi-year study of lower tropospheric aerosol variability and systematic relationships

J. P. Sherman et al.

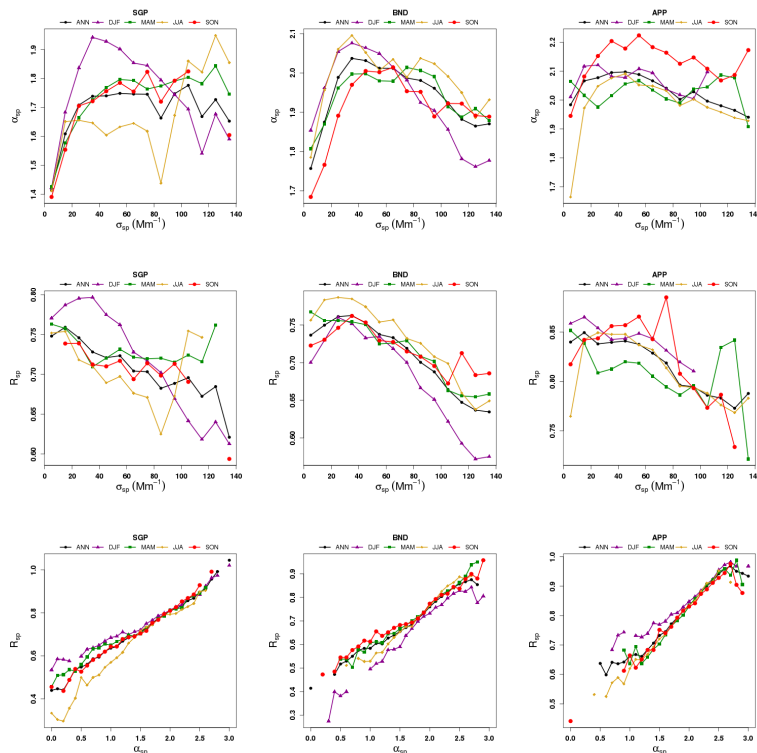


**Figure 11.** Mean scattering Ångström exponent ( $\alpha_{sp}$ ) and sub-micrometer scattering fraction ( $R_{sp}$ ) vs. scattering coefficient ( $\sigma_{sp}$ ) and mean  $R_{sp}$  vs.  $\alpha_{sp}$  for individual seasons and full annual cycles at SGP, BND, and APP over the years 2010–2013. Months comprising the seasons are DJF (winter), MAM (spring), JJA (summer), and SON (fall). The “ANN” curve in each plot represents the curve for all seasons. The mean values were calculated over  $10 M m^{-1}$   $\sigma_{sp}$  bins and over  $0.1 \alpha_{sp}$  bins. All values are for the  $PM_{10}$  size cut.  $R_{sp}$  and  $\sigma_{sp}$  are given for a wavelength of 550 nm and  $\alpha_{sp}$  and  $\alpha_{ap}$  are calculated using the 450/700 nm wavelength pair.

## A multi-year study of lower tropospheric aerosol variability and systematic relationships

J. P. Sherman et al.

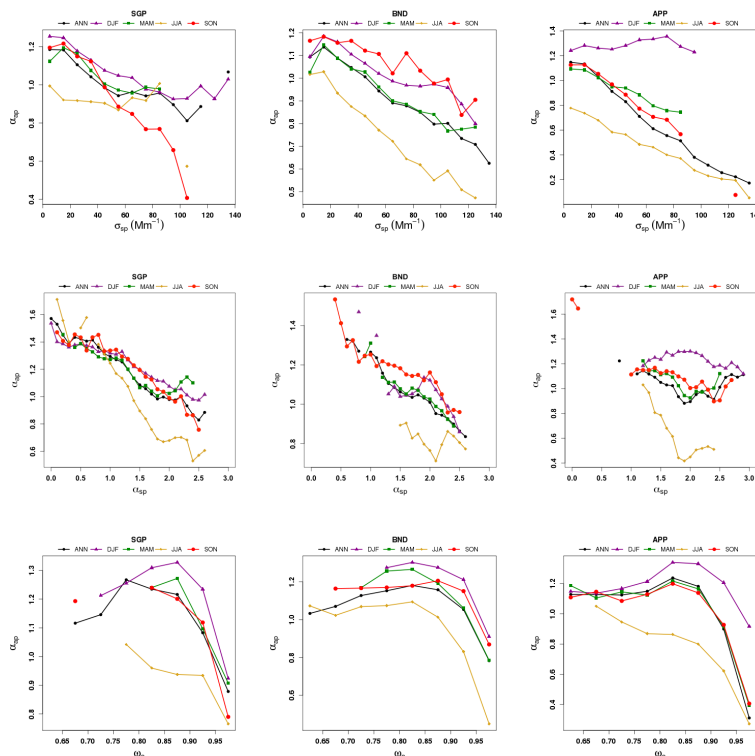


**Figure 12.** Mean absorption Ångström exponent ( $\alpha_{ap}$ ) vs. scattering coefficient ( $\sigma_{sp}$ ), scattering Ångström exponent ( $\alpha_{sp}$ ), and single-scattering albedo ( $\omega_0$ ) for individual seasons and full annual cycles at SGP, BND, and APP over the years 2010–2013. Months comprising the seasons are DJF (winter), MAM (spring), JJA (summer), and SON (fall). The “ANN” curve in each plot represents the curve for all seasons. The mean  $\alpha_{ap}$  values were calculated over  $10 \text{ M m}^{-1}$   $\sigma_{sp}$  bins,  $0.1 \alpha_{sp}$  bins, and  $0.05 \omega_0$  bins. All values for  $\sigma_{sp}$  and  $\omega_0$  are given for a wavelength of 550 nm and  $\alpha_{sp}$  and  $\alpha_{ap}$  are calculated using the 450/700 nm wavelength pair.

[Title Page](#)
[Abstract](#)
[Introduction](#)
[Conclusions](#)
[References](#)
[Tables](#)
[Figures](#)
[Back](#)
[Close](#)
[Full Screen / Esc](#)
[Printer-friendly Version](#)
[Interactive Discussion](#)